Tuijin Jishu/Journal of Propulsion Technology
ISSN: 1001-4055
Vol. 45 No. 2 (2024)

Optimization and ANN Modelling for Performance and Emissions Prediction of a Biodiesel-Diesel Blend Engine with EGR using Response Surface Methodology

Rajesh Kumar Saluja[a], Dekkala Vinay[a], Narender Singh[a], Radhey Sham[b], Freddie Inambao[c*]

[a] Amity Institute of Aerospace Engineering, Amity University-Uttar Pradesh, Noida, India.

[b] Chandigarh College of Engineering &Technology, Chandigarh, India.

[c] University of KwaZulu-Natal, Durban, South Africa.

[c*]Corresponding author: inambaof@ukzn.ac.za

Abstract

This study evaluates the effects of Jatropha and Karanja biodiesels and their blends on a diesel engine's fuel economy, performance, and exhaust emissions. Response Surface Methodology was applied to model engine responses using four key input parameters: blend percentage, load, injection timing, and Exhaust Gas Recirculation. RSM projected multiple Pareto-optimal solutions through multi-objective optimization and contour plots. The study investigated important engine responses like Brake Thermal Efficiency, Brake Specific Fuel Consumption, HC emissions, smoke, NOx, and EGR. RSM models for Jatropha biodiesel and blends displayed high R^2 values, ranging from 0.93 to 0.99. Similarly, Karanja biodiesel and blends exhibited R^2 values ranging from 0.94 to 0.98. The results indicate that all tested fuels provided accurate approximations for the engine responses. Furthermore, an Artificial Neural Network model was developed to predict input parameters based on desired performance and emission constraints. The ANN approach proved effective in predicting engine responses based on operating conditions, injection system parameters, and exhaust gas recirculation.

Keywords: Biodiesel, Optimization, Biodiesel blends, Response Surface Methodology, Artificial Neural Network.

1 Introduction

Biofuels have emerged as a viable alternative to fossil fuels and have been in use for several years now. These fuels are derived from plant matter and are considered low-carbon. It is predicted that biofuels will witness a significant rise in demand over the next five years, thereby reducing our dependence on fossil fuels. Biofuels are known to burn more efficiently and emit fewer pollutants and greenhouse gases when compared to conventional fossil fuels. The availability of petroleum resources is limited, and they are primarily concentrated in specific geographical regions. Furthermore, the demand for petroleum-based fuels is continuously increasing, leading to a corresponding rise in prices [1]. Petro-diesel is known to emit a significant amount of pollutants and greenhouse gases, such as carbon monoxide (CO), hydrocarbons (HC), particulate matter (PM), sulphur dioxide (SO_2), and nitrogen oxides (NOx), which have adverse health and environmental effects. The harmful impacts of these contaminants on human health have been established in previous studies (Silverman et al., 2012) [2]. On the other hand, biodiesel exhibits similar properties to diesel fuel in terms of cetane number, heating value, long-chain unbranched hydrocarbons, etc. [3-5].

Biofuels are considered an eco-friendly and convenient alternative to conventional fuels as they promote energy security, support economic development, reduce greenhouse gas emissions and other pollutants, maintain energy balance, and are biodegradable and recyclable [6]. Numerous studies have investigated the advantages, disadvantages, and characteristics of biofuels [3-7]. These fuels can be produced using edible vegetable oils such as sunflower, palm, peanut, soybean, coconut, and rapeseed, as well as non-edible vegetable oils such as Jatropha, Karanja, algae, halophytes, and sea mango. Additionally, biofuels can also be made from recycled or waste oils and animal fats such as cow tallow, yellow grease, chicken fat, and fish oil by-products.

Figure 1. shows the overview of the common method for the production of biodiesel from the feed stock. It is popularly known as trans-esterification process.

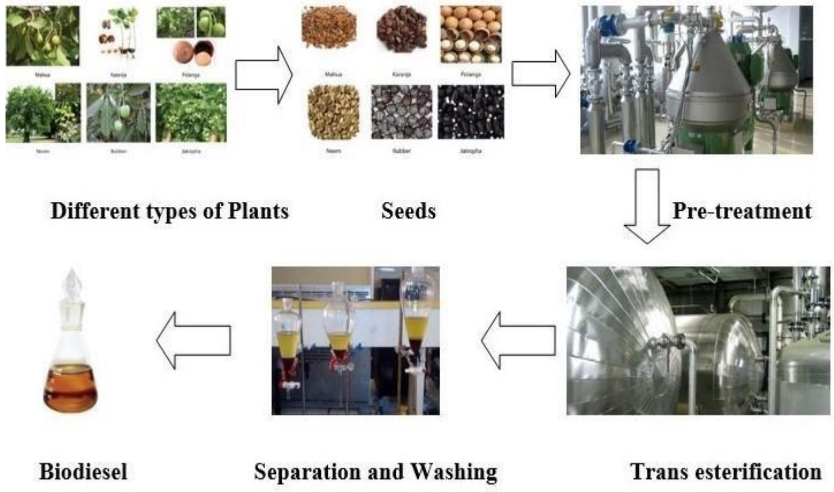

Fig. 1 Biodiesel production from feedstock via trans-esterification process [8].

Over the past few years, the use of biodiesel as a diesel engine fuel has gained significant attention, with several investigations examining its performance, emission analysis, stability, and efficiency properties. The aim has been to achieve higher Brake Thermal Efficiency (BTE) and lower Brake Specific Fuel Consumption (BSFC) to reduce fuel consumption and greenhouse gas emissions. Researchers have conducted tests to determine if biodiesel and its blends with diesel can outperform pure diesel in terms of efficiency [9-12].

Studies have shown that biodiesel blends can achieve higher efficiency levels than pure diesel. For instance, Devarajan et al. [13] evaluated neat biodiesel and heptanol biodiesel blends in a diesel engine. The study showed that as the heptanol level in the heptanol and biodiesel blends increased, the BSFC decreased, and the BTE increased. The engine exhibited a maximum reduction in BSFC of 0.19 kg/kWh and a 1.7 percent increase in BTE when fueled with the 228 M80H20 blend under naturally aspirated conditions. Similarly, several studies have found that using biodiesel blends improves BTE [7,14].

However, several studies have reported a decline in efficiency with the use of biodiesel. Patidar et al. [15] studied the performance and durability of a single-cylinder direct injection diesel engine running on a biodiesel-diesel fuel blend that was water emulsified. According to the findings, in comparison to HSD, PB20S10W and B20 showed higher BSFC. PB20S10W and B20 had 7.40 percent and 3.23 percent greater BSFC than HSD at 75 percent load, respectively. Pal et al. [16] conducted an experimental and numerical study on Jatropha biodiesel and found that, as compared to conventional diesel engines, BTE lowered as biodiesel share in blends increased. The amount of biodiesel in blended fuels enhances the BSFC. The usage of Jatropha biodiesel, which has a higher oxygen content, resulted in an increase in NOx emissions, according to this study. However, when compared to pure diesel metrics remained inferior at full loads [8]. Due to the combined effect of higher viscosity and lower calorific value, BSFC increased with the addition of biodiesel to the mix during full load circumstances, resulting in a lowered BTE than diesel fuel [7, 17].

Numerous studies [1-15] have concluded that most of the emissions decrease but there is significant increase in NOx emissions. Agarwal et al. [37] investigated that biodiesel reduced PM mass emissions, which have lower environmental and health-related toxicity. Dincer [38] investigated the effect of biodiesel and found that total hydrocarbon emissions (a significant element in the localized production of smog and ozone) from biodiesel are on average 67 percent lower than diesel fuel. However, some researchers have come up with some suggestions to lower NOx emissions, and the proof shows that Radhey Sham et al. [18] conducted an experimental investigation study on the impacts of employing EGR (exhaust gas recirculation) in a directed injection diesel engine. As a result, it was observed that when EGR is larger than 16 percent, NOx emissions tend to decrease, and that cooling EGR plays an essential role in lowering NOx emissions. Kumar et al. [19] conducted a similar experiment on a CI engine using a 20 percent blend of Jatropha biodiesel. At maximum load condition, NOx was reduced by 20.8 percent and 36.9 percent at 10 percent and 20 percent EGR, respectively.

The performance and emission characteristics of the biodiesel also depend on the feedstock of the biodiesel, which may be edible or non-edible vegetable oil. In the Indian context, the non-edible vegetable oils produced from Jatropha and Karanja have great suitability [19, 20]. Some studies [4, 19-22] have investigated the production and attributes of Jatropha biodiesel because it has a higher percentage of methyl esters [8]. Aparna Singh et al. [23] investigated biodiesel synthesis using heterogeneous catalysts, as well as the use of Taguchi robust design and response surface methods to improve diesel engine performance when employing Jatropha biodiesel blends. When compared to baseline mineral diesel, B30 (30 percent biodiesel+70 percent diesel) has been proven to function similarly. As a result, biodiesel made from Jatropha curcas oil employing a heterogeneous catalyst can be used as a fuel blend with diesel in normal diesel engines without requiring any engine modifications. The Use of Jatropha Biodiesel as a Future Sustainable Fuel was also studied by Datta et al. [11].

It is important to note that the impact of biodiesel on engine efficiency and emissions can vary depending on several factors, including the type and quality of biodiesel used, the engine type, operating conditions, and fuel blend ratios. Overall, while biodiesel has the potential to improve engine efficiency and reduce emissions, further research is needed to fully understand its impact and to develop strategies to mitigate its potential negative effects, such as increased NOx emissions. Additionally, it is important to consider the sustainability of biodiesel production and the potential impact on land use, food security, and biodiversity. From the literature review it has been observed that though there have been numerous performance and emission studies on the use of biodiesel yet there is very less literature available to find the combined effect of various engine input parameters. Also, very few studies have done the optimization under various operating and performance parameters. Therefore, the present work has been undertaken to bridge the mentioned gap. The main focus of this study is on the biodiesel produced from non-edible oils from Jatropha and Karanja, which have been identified as prospective biodiesel sources in India's biodiesel mission [10].

The comprehensive and specific objectives of the present work are:

1. Investigating the combined effects of load and injection timing, blending, and EGR on diesel engine performance and emissions to provide a better understanding of how these factors interact and affect engine operation.
2. Comparing the performance of biodiesel from Jatropha and Karanja in order to give insight into which of these fuels is more suitable for use in diesel engines.
3. Developing a mathematical model and an ANN-based predictive model to enable the prediction of engine performance and emissions under different operating conditions and making it easier to optimize engine design and operation.

Overall, these objectives will contribute to the advancement of knowledge and understanding of the use of biodiesel in diesel engines, which can lead to improved engine performance and reduced emissions.

2. Materials and Methodology:

2.1 Biodiesel Blend preparation

The biodiesel samples were produced from Jatropha and Karanja oils using a catalytic trans-esterification process with KOH as the catalyst. Commercial diesel was obtained from a local fuel station and was blended with the biodiesel samples to create blends with 20% and 50% biodiesel content. The blends that were tested included Diesel, KB20, KB50, KB100, JB20, JB50, and JB100. The qualities of each blend and biodiesel sample were evaluated according to applicable standards, and the results are shown in Table 1.

Table 1. The physicochemical properties of biodiesel blends

Properties	Test Methods	Diesel	KB20	KB50	KB100	JB20	JB50	JB100
Density (Kg/m^3)	ASTM D 4052	844	856	868	891	852	863	878
Kinematic Viscosity @40^o C (cSt)	ASTM D 445	3.84	4.10	4.68	5.64	3.97	4.35	5.11
Gross Calorific Value (MJ/Kg)	ASTM D 240	44.3	42.8	41.6	38.1	43.08	42.37	39.2
Net Calorific Value (MJ/Kg)	-	41.42	39.5	38.7	34.8	40.2	39.1	36.3

2.2 Engine set-up

The study employed a Kirloskar CAF1 single cylinder DI engine with a rated power of 4.5 kW and a constant speed of 1500 rpm. The engine's parameters are listed in Table 2, and its set-up schematic is depicted in Figure 2. Two storage tanks, one for diesel and one for biodiesel, were attached to the engine. The engine was also connected to an alternator whose supply was coupled to a control panel with a total of 4.5 kW load lamps. The control panel also included a digital temperature indicator, a digital voltmeter, and a digital ammeter. To detect the exhaust gas temperature, a digital temperature indicator was connected to the sensor at the engine's exhaust manifold. Smoke opacity was quantified using the AVL 437 smoke analyzer, while unburnt HC and NOx emissions were measured using the AVL digas 4000 gas analyzer. Injection timing was determined using the spill approach. Load cells were switched according to the desired value to vary the load. Before testing biodiesels or blends, the engine was run on diesel first, then the biodiesel tank's fuel valve was closed, and the biodiesel tank's fuel valve was opened. Data were taken only after ensuring that the engine was functioning under constant conditions to allow for easy comparison. For each fuel, readings were taken in triplicate under each condition, and the average measurement was used in the computations.

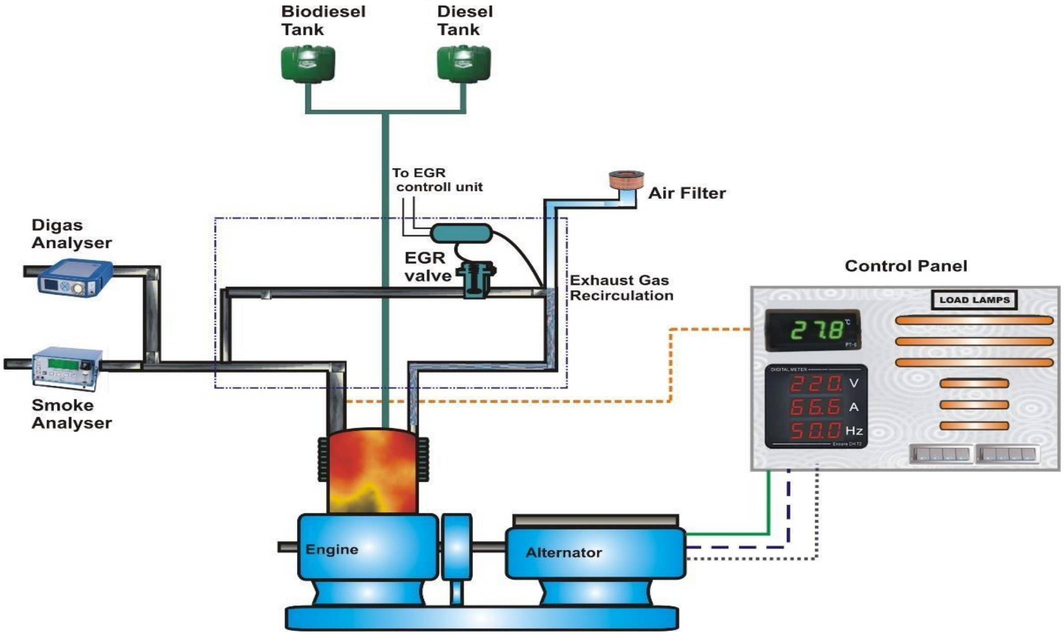

Figure 2. Schematic of Engine set up.

2.3 Exhaust Gas Recirculation

EGR is a method of reducing NOx emissions. Since, the use of biodiesel raises NOx emissions in the engine, trials were conducted with EGR. The impact of EGR on BSFC and BTE, as well as on exhaust gas emissions (smoke, HC, and NOx), has been thoroughly explored. The EGR system was connected to the engine during the investigation. The studies were conducted with 10% and 20% EGR, and the results were compared to those conducted without EGR.

For the identical operating conditions, the volume flow rate was measured with exhaust gas recirculation (V_2) and without exhaust gas recirculation (V_1), and the percentage of exhaust gas recirculation was determined as follows:

$$\% \text{ EGR} = (V_2 - V_1)/(V_1) \times 100\% \quad (1)$$

The engine was run under different biodiesel load conditions, and the effects of EGR on various engine characteristics were investigated by analysing the output responses.

Table 2. Technical specifications of the engine

Engine manufacturer	Kirloskar Oil Engines Limited, Rajkot (India)
Engine type	Single cylinder, vertical, 4- stroke diesel engine
Type of cooling	Air cooled
Bore and stroke (mm)	80x110
Maximum rated speed (RPM)	1500
Brake horsepower (BHP)	6HP (4.41 KW) at 1500 RPM
Compression ratio	17.5: 1
Type of injection	Direct injection
Injection timing	23° btdc
Lubrication oil	SAE 30/SAE 40
Governing class	“A2/B1”

3. Results and Discussion

3.1 Performance and emission analysis

Brake specific Fuel Consumption

Upon analysis results, it was observed that an increase in EGR percentage from 0 to 20% leads to an increase in BSFC for all fuels and loads. This can be attributed to the depletion of oxygen in the input mixture due to the presence of Exhaust Gas Recirculation, leading to improper combustion. The impact of EGR on BSFC varies based on the type of fuel, with diesel fuel being affected the most and pure biodiesel being affected the least due to its oxygen content. However, the effect of EGR on all fuels decreases at a load of 40%. This could be due to the accumulation of oxygen during combustion because of the reduced fuel intake in the combustion chamber.
Figures 3a-3c show the variation in BSFC with a change in EGR for a delayed injection of 180 btdc, while Figures 4a-4c illustrate the fluctuation of BSFC at conventional injection timing of 230. Figures 5a-c depict the influence of EGR on BSFC btdc at advanced injection timing of 280 btdc for different loads. Results indicate that the BSFC was lower at 70% loads and 10% EGR than at 40% load, under both normal and advanced injection time. This could be attributed to the possibility of unburned fuel particles returning with the exhaust gases at 10% EGR. Combustion also improves slightly due to sufficient oxygen and time for mixing, resulting

in a decrease in BSFC. However, the BSFC shows an increasing trend with EGR % when injection timing is delayed. This may be due to the reduced time available for mixing, as the injection start time is delayed.

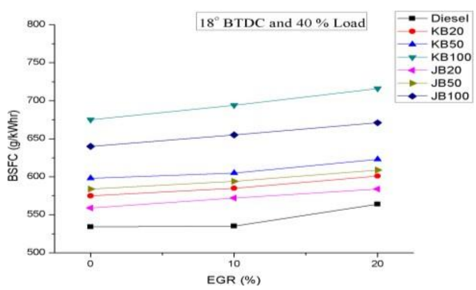

Figure 3a. 40% load

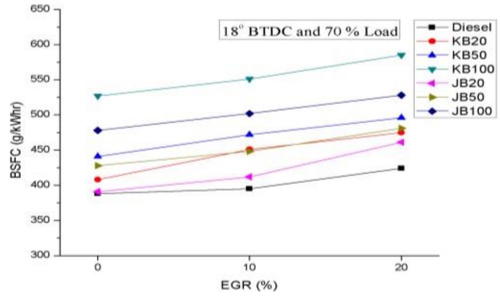

Figure 3b. 70% load

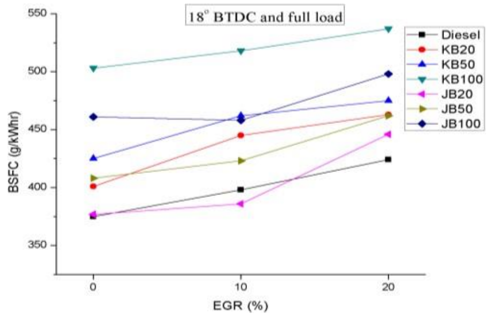

Fig 3c. Full load

Fig. 3. Effect of EGR, load and blending on BSFC at retarded injection timing (18^{o} btdc)

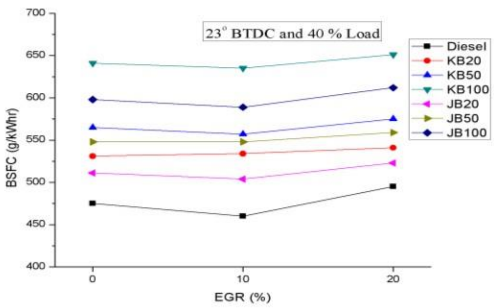

Fig. 4a. 40% load

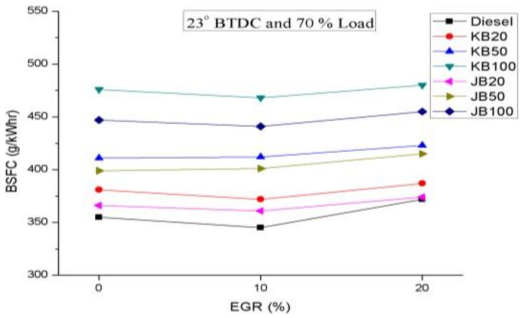

Fig. 4b. 70% load

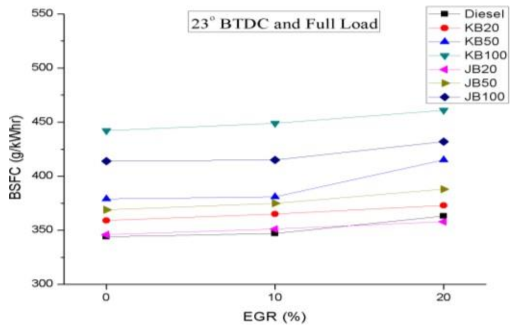

Fig. 4c. Full load

Fig. 4 Effect of EGR, load and blending on BSFC at Normal injection 23^{o} btdc.

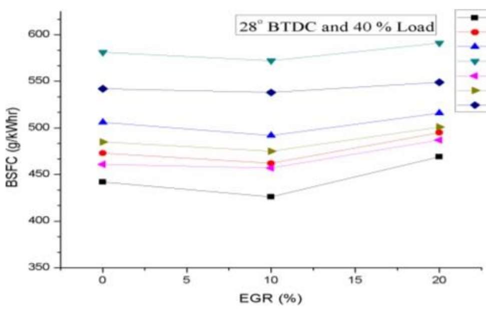

Fig. 5a. 40% load

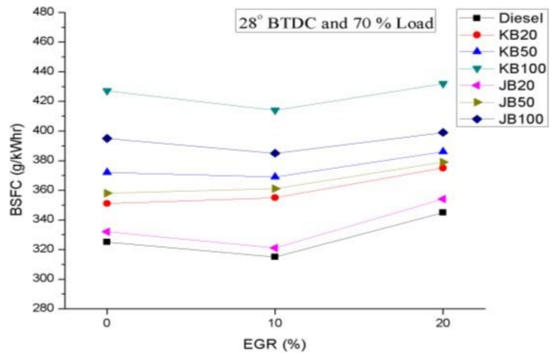

Fig. 5b. 70% load

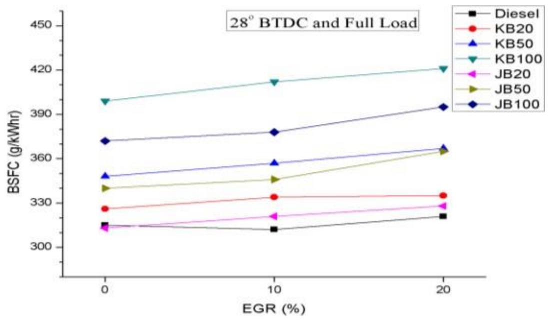

Fig. 5c. Full load

Fig. 5 Effect of EGR, load and blending on BSFC at Advanced injection (28° btdc).

Brake Thermal Efficiency (BTE)

The graphs in Figures 6a-6c illustrate how the Brake Thermal Efficiency (BTE) changes with Exhaust Gas Recirculation (EGR) for normal injection timing. At full loads, increasing EGR slightly decreases BTE, but at low and mid loads, a 10% EGR can slightly improve efficiency. This is due to the decrease in Brake Specific Fuel Consumption (BSFC) caused by the recirculation of unburned fuel particles, which was explained in the previous section. EGR has a greater impact on diesel fuel and blends than pure biodiesel.

The impact of EGR on BTE during delayed injection can be observed in Figures 7a-7c, where EGR reduces efficiency at all loads. This is likely due to reduced timing for mixing air and fuel in the combustion chamber. At full load, EGR reduces efficiency quickly.

Finally, the effect of EGR on efficiency at advanced injection can be seen in Figures 8a-8c. For almost all fuels, efficiency improves at low loads when EGR is set at 10%.

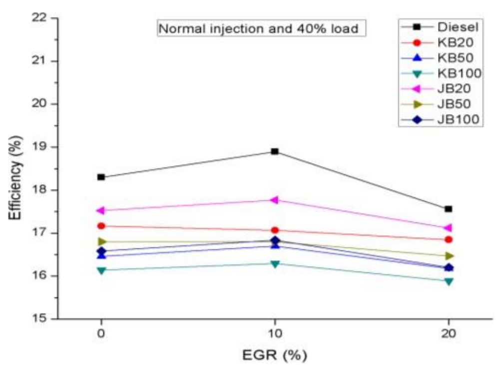

Figure 6 a. 40% load

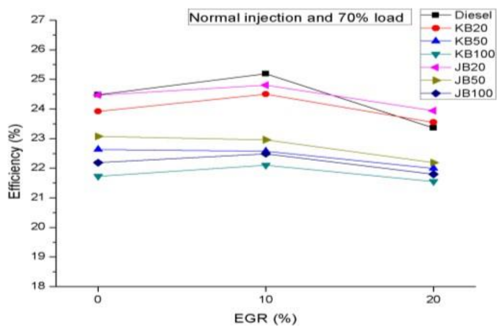

Figure 6 b. 70% load

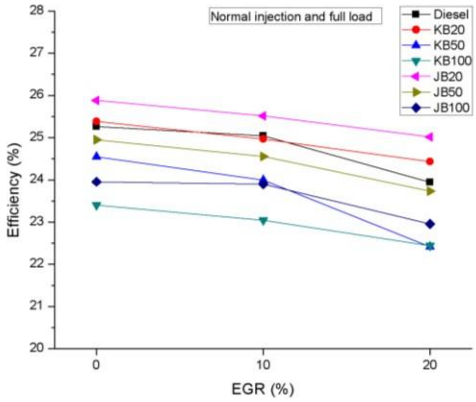

Figure 6 c. Full load

Figure 6. Effect of EGR, load and blending on BTE at Normal injection

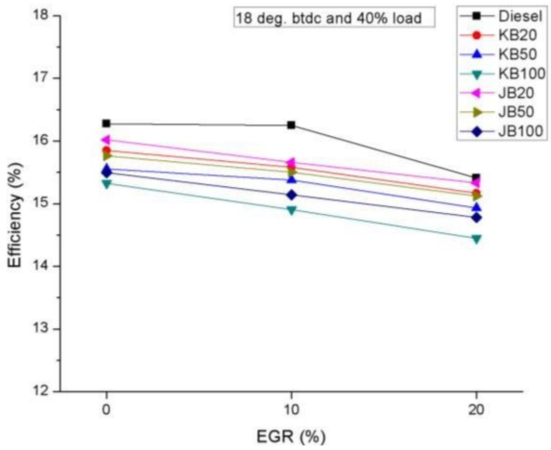

Figure 7a. 40% load

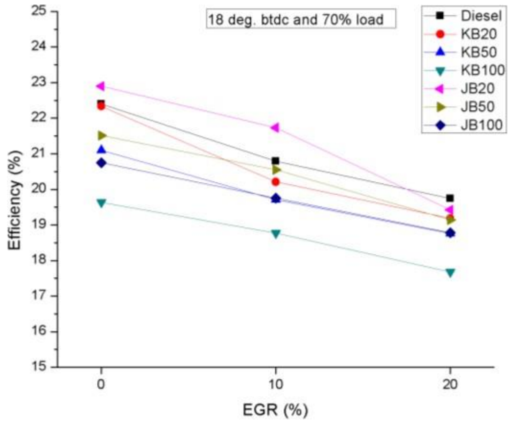

Figure 7b. 70% load

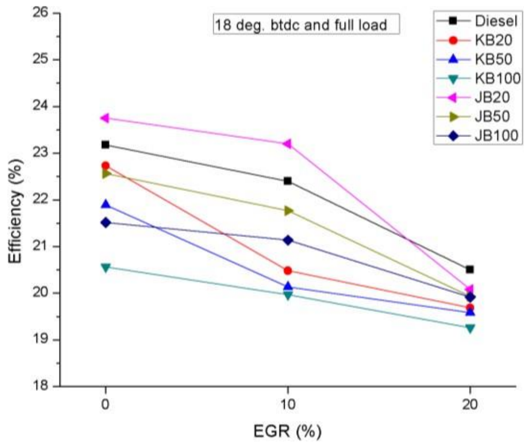

Figure 7c. Full load

Figures 7 (a-c) Effect of EGR, load and blending on BTE at retarded injection.

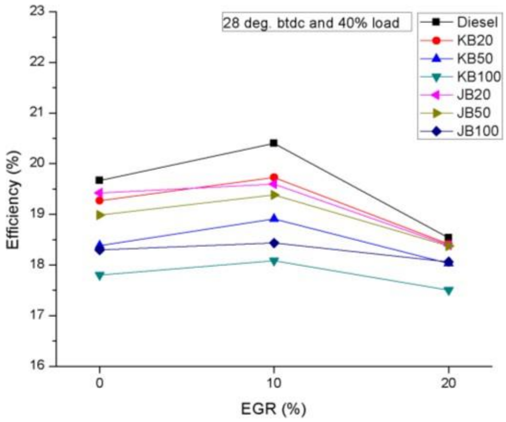

Figure 8 a. 40% Load

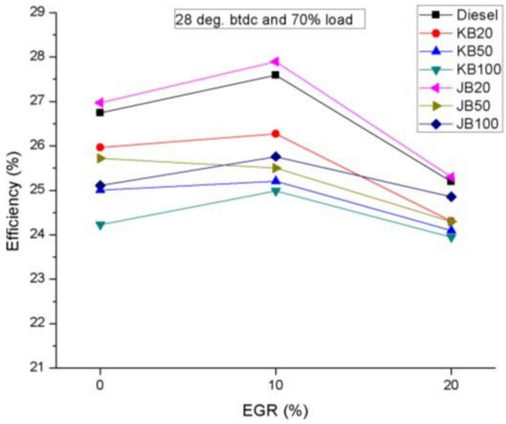

Figure 8 b. 70% Load

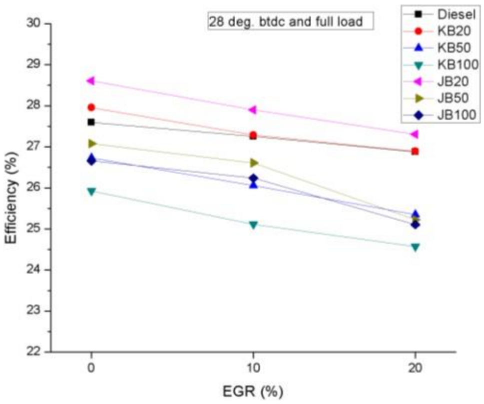

Figure 8 c. Full Load

Figures 8(a-c) Effect of EGR, load and blending on BTE at advanced injection timing (28^o btdc)

Smoke Emissions

The use of Exhaust Gas Recirculation (EGR) was found to increase smoke opacity, as smoke emissions rose with increasing loads and EGR percentages. When EGR was increased from 10% to 20%, the smoke level increased more significantly than when it was increased from 0% to 10%. This could be due to the larger volume of recirculated exhaust within the combustion chamber, which reduces the available oxygen supply. Since biodiesels contain oxygen, the increase in smoke was more prominent in diesel fuel than in biodiesels. The impact of increased EGR was more pronounced at full load compared to low and mid loads, likely due to higher fuel consumption for combustion. The trends in smoke variation with changing injection timing were similar, as shown in Figures 9 (a-c), which depict the changes in smoke opacity with EGR at various loads and injection rates.

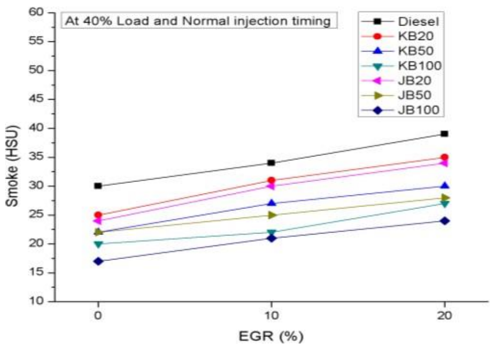

Figure 9 a. 40% Load

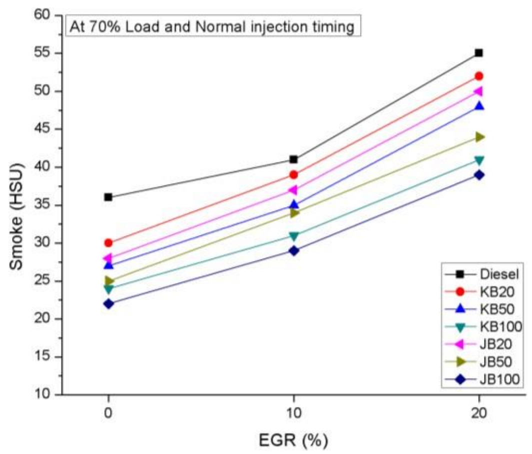

Figure 9 b. 70% Load

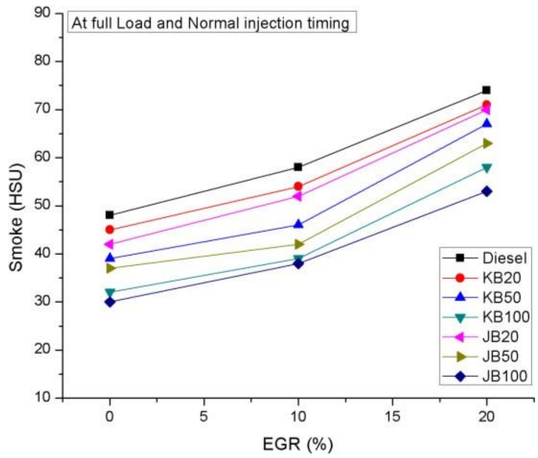

Figure 9c. Full Load

Figures 9(a-c) Effect of EGR, load and blending on Smoke emissions at Normal injection timing (23^0 btdc)

Unburnt Hydrocarbon (HC) Emissions

Figures 10 (a-c) demonstrate how Exhaust Gas Recirculation (EGR), load, and blending affect the hydrocarbon (HC) emissions for all the fuels tested at normal injection. The results indicate that increasing EGR leads to higher Unburned Hydrocarbon (UBHC) emissions. This is due to the dilution of the intake mixture and a subsequent decrease in oxygen content. This causes the formation of a locally over-rich mixture, which slows down the combustion reactions and leads to incomplete combustion. Furthermore, at a given volume, the exhaust gases in the intake mixture lower the temperature and pressure, resulting in a longer ignition delay period and increased HC emissions. The increase in HC emissions was found to be greater for diesel than pure biodiesels between 10-20% EGR. For most fuels, UBHC emissions increase linearly at full loads.

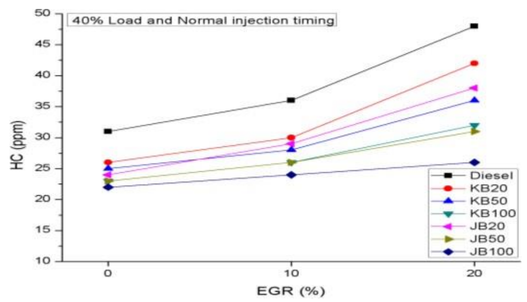

Figure 10a. 40% Load

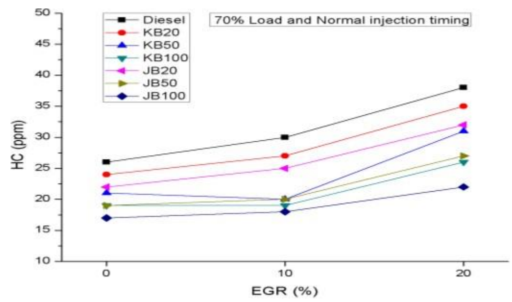

Figure 10b. 70% Load

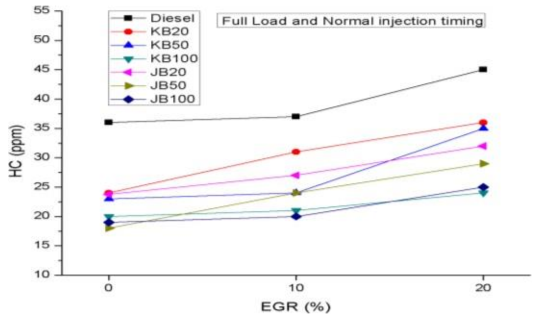

Figure 10 c. Full Load

Figures 10(a-c) Effect of EGR, load and blending on HC Emissions at Normal injection timing.

Exhaust Gas Temperature (EGT)

The results indicate that exhaust gas temperature (EGT) increases with increasing engine load for all the tested fuels. The decreased thermal efficiency of biodiesels and their blends compared to fossil diesel results in increased heat loss in exhaust gases and fuel consumption. This increased fuel consumption leads to a rise in engine cylinder temperature and subsequently, exhaust temperature. Additionally, greater heat loss occurs in exhaust gases with an increase in engine load. Biodiesel blends display higher exhaust gas temperatures than fossil diesel across the entire engine load range. EGT decreases as EGR percentage increases for all the fuels tested. This could be attributed to the reduced availability of oxygen for fuel burning. However, at 10% EGR, where combustion is enhanced and BSFC slightly decreases, EGT still

decreases, which could be due to the higher specific heat of a mixture of fresh air and exhaust gases. Figures 11 (a-c) illustrate the impact of load, blending, and EGR at normal injection timing.

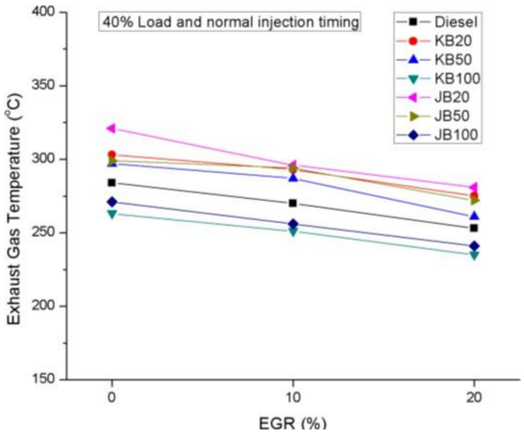

Figure 11a. 40% Load

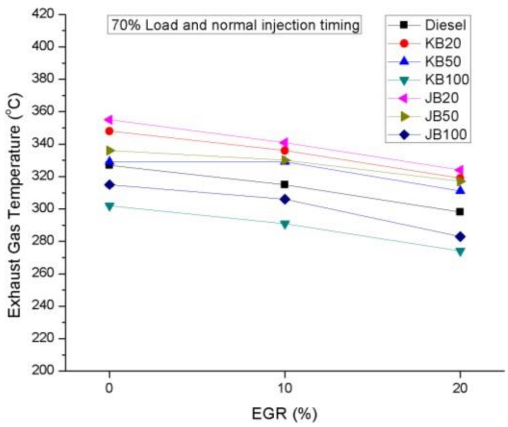

Figure 11b. 70% load

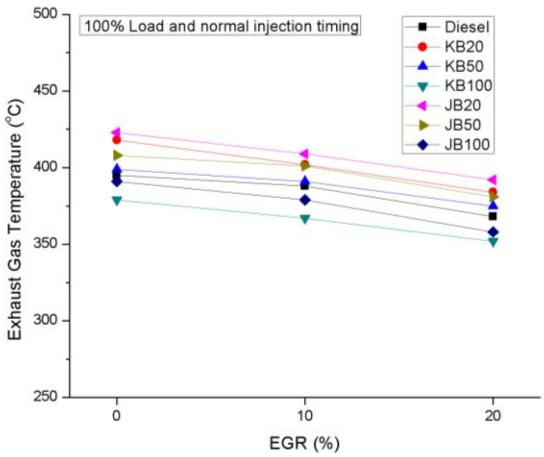

Figure 11c. Full Load

Figures 11(a-c) Effect of EGR, load and blending on EGT at Normal injection timing

NOx emissions

NOx emissions are a significant environmental concern in diesel engines, as they contribute to the formation of smog and acid rain. EGR has become a popular technique for reducing NOx emissions in diesel engines. When exhaust gases are recirculated into the engine's intake, the combustion temperature is lowered, resulting in lower NOx emissions. The decrease in NOx emissions with increasing EGR is nearly linear. Higher EGR rates have been found to result in greater reductions in NOx emissions at high loads than at low loads.

The impact of EGR on NOx emissions was more significant with biodiesel than with diesel. This is because biodiesel contains oxygen, which leads to greater formation of NOx. The reduction in NOx emissions with increasing EGR was more significant with biodiesel than with diesel. The findings suggest that EGR can be an effective technique for reducing NOx emissions in diesel engines, especially when using biodiesel. Figures 12 (a-c) demonstrate the impact of EGR on NOx emissions at normal injection timing.

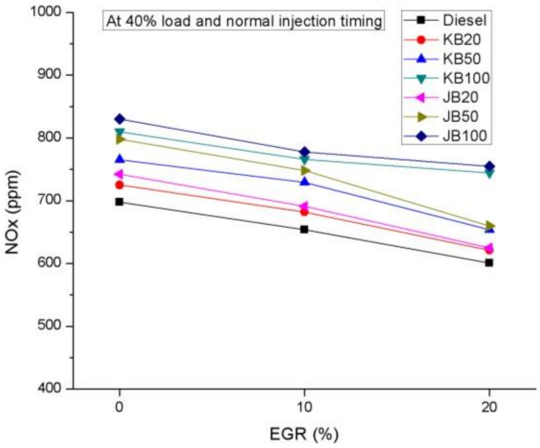

Figure 12a. 40% Load

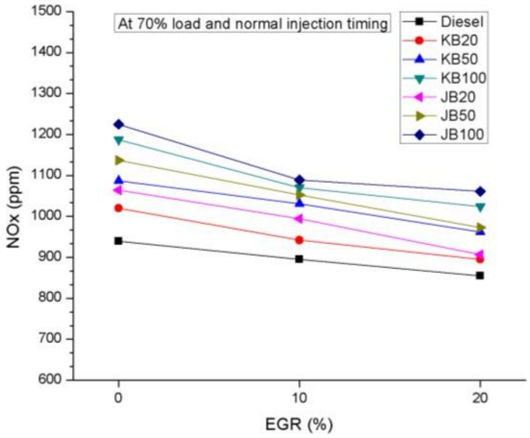

Figure 12b. 70% Load

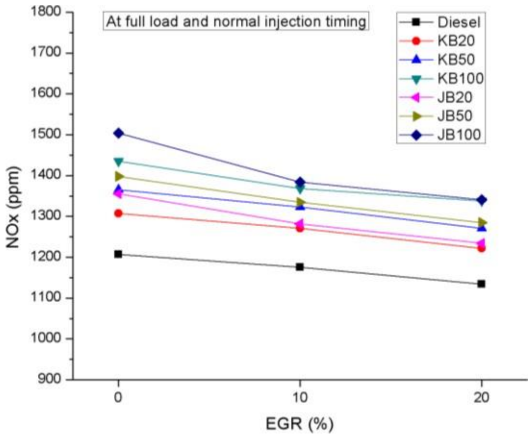

Figure 12 c. Full Load

Figure12(a-c) Effect of EGR, load and blending on NOx emissions at Normal injection timing.

3.2 Statistical analysis and Optimisation

In this study, the impact of various parameters such as blends, load, injection time, and EGR on BSFC, BTE, smoke, UBHC, EGT, and NOx were investigated through statistical analysis. To achieve this, the experimental results were analyzed using the Analysis of Variance (ANOVA) method, and a multi-objective problem was created. Design Expert 12 software was used for the optimization problem, where models for each parameter were created for Jatropha biodiesel, Karanja biodiesel, and their corresponding blends. The multi-objective optimization was then performed using these models, and the influence of all the parameters was analyzed through response surface plots. These plots showed the combined and individual effects of each parameter. Finally, the optimum solutions were determined and presented graphically through the models created.

Optimisation of Engine Operating parameters

The primary aim of this study is to enhance the operational parameters of the engine, which include blends, load, injection timing, and EGR, to achieve optimal performance in terms of thermal efficiency, BSFC, smoke, HC emissions, EGT, and NOx. Optimization problems can be classified into two categories: single-objective and multi-objective. Single-objective problems involve maximizing a single function, whereas multi-objective problems require the optimization of multiple objective functions. Since this study involves six output parameters, it requires a multi-objective optimization approach, where we need to minimize or maximize several objective functions. Generally, multi-objective optimization can be described as the process of minimizing or maximizing multiple objective functions simultaneously given by the following equation [44]:

$$\begin{aligned} &\text{Minimize/Maximize} && f_a(x), && a = 1,2,\ldots,A; \\ &\text{Subject to} && g_j(x) \geq 0, && j = 1, 2, \ldots, J; \\ & && h_k(x) = 0, && k = 1, 2, \ldots, K; \\ & && x_i^{(L)} \leq x_i \leq x_i^{(U)}, && i = 1,2,\ldots, n. \end{aligned} \tag{2}$$

A solution vector x comprises n choice variables and is represented as $x = (x_1, x_2, \ldots x_n)T$. The decision variable space is constrained by variable bounds that limit each decision variable x_i to an upper $x_i(U)$ and lower $x_i(L)$ bound. Constraint functions are expressed as $g_j(x)$ and $h_k(x)$.

In this study, the multi-objective optimization problem was solved using the Design-Expert 12.0.0 software package, which utilizes desirability functions to overcome optimization challenges. Each response Y_i is transformed into an individual desirability function d_i that varies across the range. The desirability function d_i takes a value between zero and one, where d_i is one when the response is at its target, and zero when it falls outside the acceptable range.

The design parameters are then selected to maximise overall desirability:

$$D = (d_1 * d_2 * \ldots * dn)1/n \tag{3}$$

Where, n is the number of responses.

If the goal for the response Y_i is a maximum value, the desirability curve is defined as:

$$d_i = [(Y_i - L_i)/(H_i - L_i)]^{wt_i} \tag{4}$$

If the goal for the response Y_i is a minimum value, the desirability curve is defined as:

$$d_i = [(L_i - Y_i)/(H_i - L_i)]^{wt_i} \tag{5}$$

Where, L_i and H_i are the lower and higher limits for the response Y_i and wt_i is the response's weight. Weights are used to highlight the target value or upper/lower bounds. Hence, when $wt_i = 1$, the di has a linear range of 0 to 1, while $wt_i > 1$ and $wt_i < 1$ are indicated as having high and low importance in the target's proximity, respectively [39]

Optimization models for Jatropha and Karanja Biodiesel blends

To solve an optimization problem, it is essential to construct a suitable model that relates the output responses to the input parameters. In this study, six models were developed for load, blend ratio, injection timing, and EGR, as there were six output variables to consider. The statistical models were built using the response surface methodology (RSM) technique, with individual models developed for the Karanja and Jatropha biodiesel blends, including a 0% blend (pure diesel) and a 100% blend (pure biodiesel).

RSM is a powerful approach that employs various mathematical and statistical tools to analyze complex systems with multiple inputs and outputs, with the ultimate goal of optimizing the system's response. Typically, RSM uses a low-order polynomial to establish a connection between the input parameters and the output response, with the polynomial being valid for some regions of the independent variables. The general equation for this polynomial can be expressed as:

$$y = \beta_0 + \beta_1 x_1 + \beta_2 x_2 + ...+ \beta_k x_k + \varepsilon \quad (6)$$

If there is a curvature in the system, a polynomial of higher degree is used. The following equation shows a second-order model:

$$y = \beta_0 + \sum_{i=1}^{k} \beta_i x_i + \sum_i \sum_j \beta_{ij} x_i x_j + \sum_{i=1}^{k} \beta_{ii} x_i^2 + \varepsilon \quad (7)$$

The models created in this study include all of the input parameters' individual terms, quadratic terms, and two-way interaction terms. The Jatropha models are shown below.

*BSFC = +393.74 -79.69*A + 44.63*B - 47.29*C + 12.38*D -8.43*AB +5.48*AC + 2.00*AD - 4.32*BC - 1.02*BD -6.58*CD +60.54*A^2 + 1.25*B^2 + 6.25*C^2 + 10.08*D^2 (8)*

*BTE = +23.55 + 3.57*A - 0.79*B +2.30*C - 0.60*D - 0.084*AB + 0.47*AC -0.25*AD -0.078*BC + 0.11* BD + 0.21*CD - 2.51*A^2 + 0.14* B^2 - 0.098*C^2 - 0.51*D^2 (9)*

SMOKE = +31.89 + 31.89 A - 7.99* B - 6.16* C + 8.35* D -1.47* AB - 1.43* AC + 4.05*AD + 0.62*BC - 0.59* BD -0.41*CD + 3.07*A^2 + 3.00*B^2 +1.08* C^2 + 1.81* D^2. (10)*

*HC = +19.03 - 1.36*A -6.98* B + 2.79* C + 5.03*D - 0.90*AB -1.08*AC -0.69*AD - 0.36*BC - 1.25*BD + 2.48*CD + 4.55*A^2 + 5.24*B^2 - 0.56*C^2 + 1.92*D^2 (11)*

*EGT = +337.40 + 56.94*A - 7.56*B + 17.83*C -13.91*D + 1.06*AB + 1.85*AC + 0.54*AD - 0.7*BC + 0.95*BD - 0.31*CD + 12.14*A^2 - 24.58*B^2 - 1.24* C^2 - 3.28* D^2 (12)*

NOx = +1061.34 +309.26 A + 88.68*B +124.29*C - 59.34*D +20.61*AB + 46.42*AC -7.06 * AD + 19.50*BC - 13.64*BD - 13.77* CD - 22.89*A^2 - 41.08*B^2 + 29.78*C^2 + 4.07* D^2 (13)*

Where, A-Load, B-Blend percentage, C-Injection timing before TDC and D- EGR.

The models for Karanja are shown below.

BSFC = +414.83 - 79.58*A + 60.91*B - 51.22*C + 12.29*D -10.00*AB + 2.31*AC + 2.04*AD - 7.02*BC - 0.60*BD - 7.04*CD + 61.17*A2 + 1.18*B2 + 8.25 * C2 + 6.21* D2 (14)

BTE = +22.75 + 3.36*A - 1.05*B + 2.35*C - 0.56*D - 0.15*AB + 0.60*AC -0.24*AD - 0.057*BC + 0.12*BD + 0.22*CD - 2.41*A2 + 0.41* B2 - 0.20*C2 - 0.28*D2 (15)

HC = +21.38 - 1.27*A - 6.57*B + 2.79*C + 5.63*D - 1.47*AB - 0.90*AC -0.98*AD - 0.74*BC - 0.97*BD + 2.40*CD + 4.65*A2 + 3.45*B2 - 1.05*C2 + 2.67* D2 (16)

SMOKE= +34.42 + 13.04*A - 6.81*B - 6.59*C + 8.64*D - 1.13*AB - 1.26*AC + 4.30*AD + 0.15*BC - 0.23*BD - 0.30*CD + 3.02*A2 + 1.77*B2 + 1.01*C2 + 2.08*D2
(17)

EGT= +329.43 + 56.10*A - 10.53*B + 17.77*C - 13.84*D + 0.39*AB + 1.31*AC + 0.25*AD - 0.054*BC + 0.80*BD - 0.67*CD + 11.57*A2 -20.65*B2 - 0.31*C2 - 3.60*D2 (18)

NOx = +1038.38 + 298.89*A + 75.48*B + 122.38*C - 55.86*D + 8.32*AB + 45.44*AC - 9.52*AD + 19.38*BC - 16.86*BD - 11.77*CD - 25.08*A2 -36.77*B2 + 43.50*C2 - 3.92*D2
(19)

Where, A-Load, B-Blend percentage, C-Injection timing before TDC and D- EGR.

Multi-objective optimisation is carried out using statistical models. To verify the fitness of the response surface models, several output responses were exhibited individually versus the two input parameters. The 3-D response surfaces reflect the combined influence of the two factors at any particular moment. These response surfaces were drawn for a wide range of combinations, from 0% (pure diesel) to 100% (pure biodiesel). Separate analyses were performed on Jatropha and Karanja biodiesel/blends. Some of the results are seen in Figures 13 – 28. Table 3 displays the lowest, maximum, and mean values of the measured responses. The R^2 value of the response surface models is also shown in the table. The R^2 value indicates how near the data set is totheitted regression line. It's also referred to as the coefficient of determination. It can be calculated using the following formula:

Coefficient of determination, R^2 = (Sum of squares due to model)/(total Sum of squares) (20)

As the total sum of squares = Sum of squares due to model + sum of squares due to residuals/ errors, therefore the equation can also be written as:

Coefficient of determination, R^2 = 1- (Sum of squares due to residuals/errors)/(total Sum of squares) (21)

R2 can be calculated using either of the following formulae. R2 = 0 means that the dependent variable cannot be predicted using the input variables, but R2 = 1 means that the error-free output response can be predicted using the input parameters. R2 = 0.9, on the other hand, shows that the output response is 90% correct and 10% unexpected.

Figures 13–28 illustrate response surface graphs and predicted vs. experimental data graphs for various combinations of input parameters to demonstrate the combined effect.

Table.3 Important statistical values for biodiesel/ biodiesel blends

	BSFC (g/kWh)		BTE (%)		Smoke (HSU)		HC (ppm vol:)		Nox (ppm vol:)	
	Karanja biodiesel blends	Jatropha biodiesel blends	Karanja biodiesel blends	Jatropha biodiesel blends	Karanja biodiesel blends	Jatropha biodiesel blends	Karanja biodiesel blends	Jatropha biodiesel blends	Karanja biodiesel blends	Jatropha biodiesel blends
Minimum	312	312	14.4	14.7	16.1	14.3	14	14	581	581
Maximum	716	671	27.9	28.6	85	85	54	53	1689	1751
Mean	456.8	439.02	21.2	21.6	40.5	38.8	28.5	27.1	1015.0	1031.1
R^2	0.98	0.99	0.98	0.98	0.98	0.98	0.94	0.93	0.98	0.99

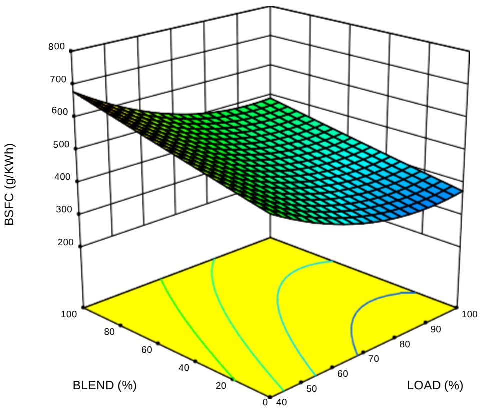

Fig. 13 Response surface of BSFC for KB100 at 0% EGR and retarded injection (18° btdc)

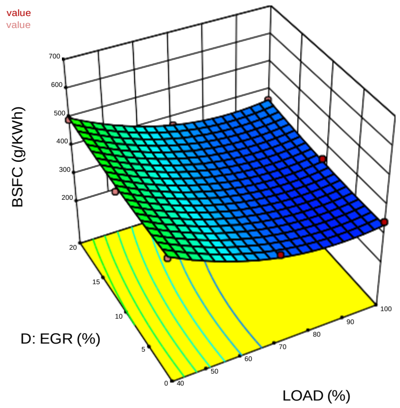

Fig. 14 Response surface of BSFC for diesel at normal injection

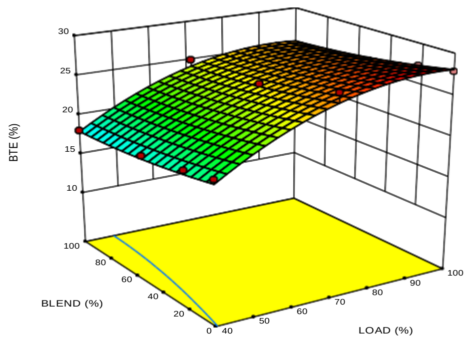

Fig. 15 Response surface of BTE for KB50 at 20% EGR

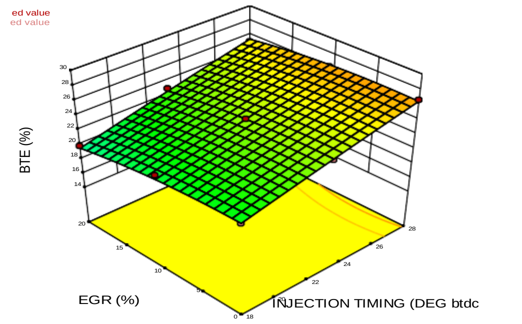

Fig. 16 Response surface of BTE for JB100 at full load

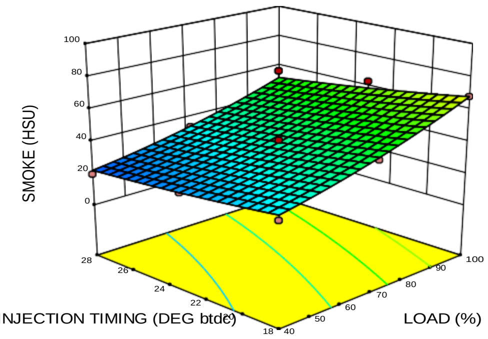

Fig. 17 Response surface of smoke for KB100 at 20% EGR

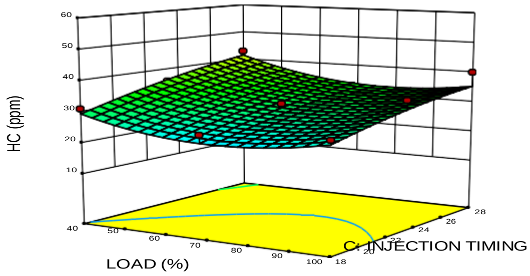

Fig. 18 Response surface of HC emissions for KB50 at 20% EGR

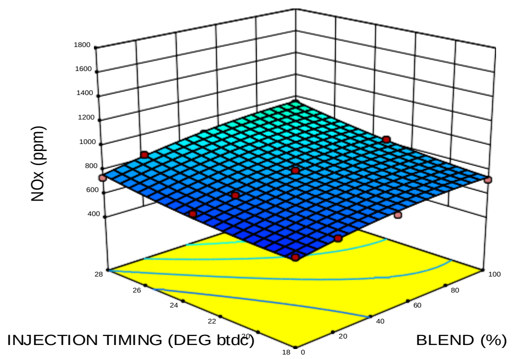

Fig. 19 Response surface of NOx for biodiesel blends at 0% EGR and 40% load

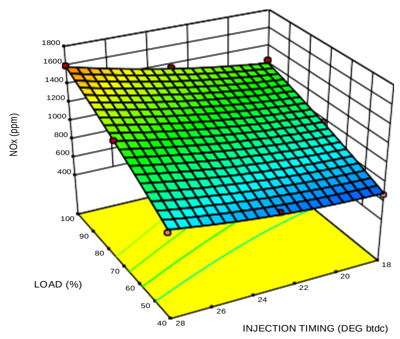

Fig. 20 Response surface of NOx jatropha for JB100 at 10% EGR

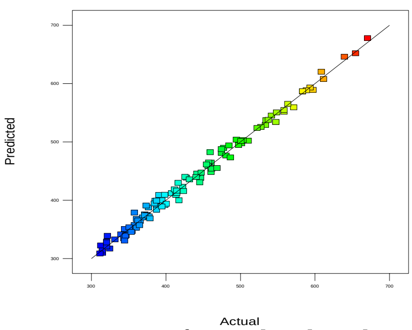

Fig. 21 Comparison of Actual and predicted values of BSFC for Jatropha biodiesel and blends (R^2= 0.99)

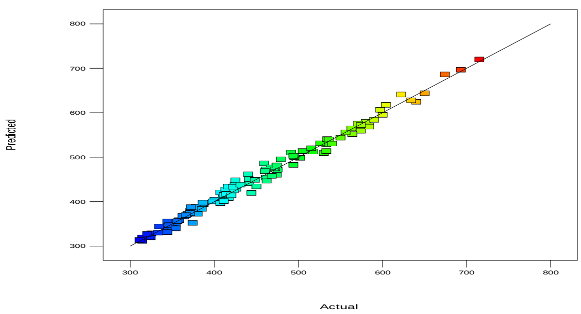

Fig. 22 Comparison of Actual and predicted values of BSFC for Karanja biodiesel and blends (R^2= 0.98)

420

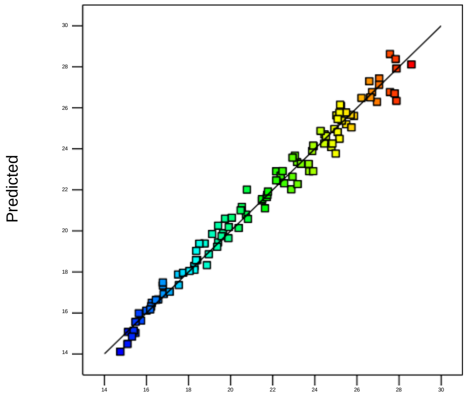

Fig. 23 Comparison of Actual and predicted values of BTE for Jatropha biodiesel blends (R^2= 0.98)

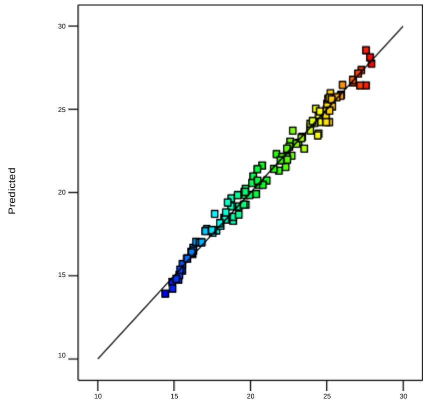

Fig. 24 Comparison of Actual and predicted values of BTE for Karanja biodiesel and and blends (R^2= 0.98)

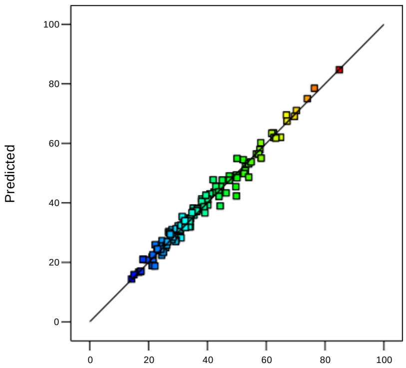

Fig. 25 Comparison of Actual and predicted values of smoke for Jatropha biodiesel and blends (R^2= 0.98)

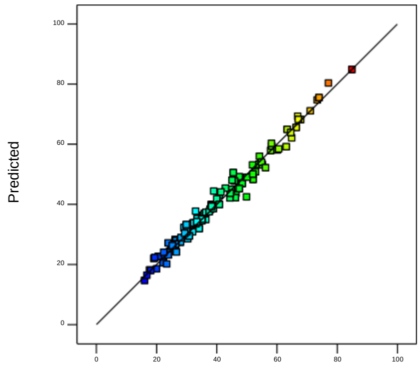

Fig. 26 Comparison of Actual and predicted values of smoke for Karanja biodiesel and blends (R^2= 0.98)

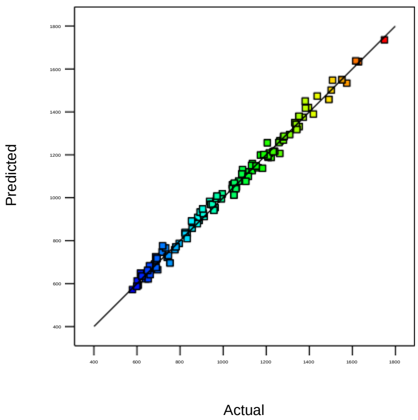

Fig. 27 Comparison of Actual and predicted values of NOx for Jatropha biodiesel and blends (R^2= 0.99)

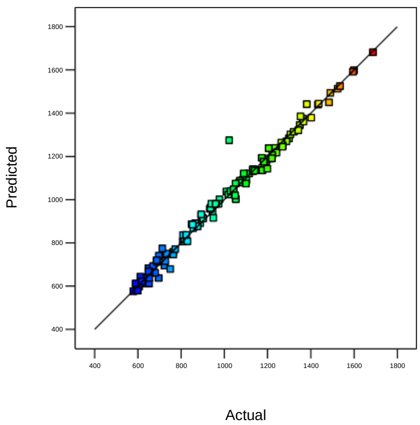

Fig. 28 Comparison of Actual and predicted values of NOx for Karanja biodiesel and blends (R^2= 0.98)

Optimisation Results

The objective of the optimization process was to identify the optimal operating parameter values for achieving the desired output conditions. The solutions that met the input parameter values for the specified output conditions were obtained by applying various constraints on the output parameters such as BSFC, BTE, smoke, HC emissions, EGT, and NOx. EGT did not have a direct impact on any of the six output responses, but it affected NOx, emissions, and performance measures. Thus, EGT was not restricted. The aim was to maximize the efficiency of the five output responses and minimize the other values. The upper limit for all parameters that needed to be minimized was set at the mean value. Design Expert 12.0 software was used to evaluate and optimize the models, which can address multi-objective optimization problems.

The input parameters were chosen during optimization to optimize overall desirability. The optimization process involved using each input parameter combination, one at a time, as the starting point for finding the best combination. Statistical models were employed to optimize each fuel mix independently. The optimization process generated a set of solutions that satisfied the specified output requirements.
The study applied the following optimization constraints for Jatropha blends and Karanja blends:

i. Maximizing BTE while minimizing each response one at a time and keeping the values of the remaining responses below their mean value.
ii. Minimizing each response one at a time while keeping all other responses within the limit.
iii. Maximizing BTE while keeping all other responses below their mean value.
iv. Minimizing two responses while keeping the others below the mean value.

Tables 4-13 list the limitations and the set of solutions for various diesel and biodiesel blends, loads, and injection start times that satisfy the specified constraints. The optimization process yielded output responses that were within the specified limits, as shown in these tables. It is important to note that while there may be multiple solutions for a given set of constraints, none of them can be deemed superior to others because they all meet the necessary requirements in the same zone. Pareto-optimal solutions are examples of this type of solution.

Table 4 Output responses constrains for minimizing NOx and maximizing BTE for Jatropha biodiesel /diesel blends

	Name	**Goal**	**Lower Limit**	**Upper Limit**
INPUT RESPONSES	LOAD	is in range	40	100
	BLEND	is in range	0	100
	INJECTION TIMING	is in range	18	28
	EGR	is in range	0	20
OUTPUT RESPONSES	SMOKE	is in range	14.36	38
	HC	is in range	14	27.1
	EGT	None	228	443
	NOx	**Minimize**	**581**	**1031.1**
	BSFC	is in range	312	439
	BTE	**Maximize**	**25**	**28.6**

Table 5. Solutions to the response constrains for minimizing NOx and maximizing BTE for diesel/ Jatropha biodiesel blends.

S. No.	LOAD	BLEND	INJECTION TIMING	EGR	SMOKE	HC	EGT	NOx	BSFC	BTE
1	68.8	2.6	25.0	2.2	33.6	27.1	336.9	1016.2	337.3	25.3
2	68.8	2.6	25.0	2.3	33.6	27.1	336.9	1016.2	337.3	25.3
3	68.7	2.6	25.0	2.3	33.5	27.1	336.8	1016.2	337.3	25.3
4	68.7	2.6	25.0	2.2	33.5	27.1	336.8	1016.0	337.4	25.3
5	68.7	2.4	25.0	2.1	33.5	27.1	336.8	1016.1	337.3	25.3
6	69.0	2.4	24.9	2.2	33.7	27.1	336.9	1016.1	337.2	25.3
7	68.9	2.3	24.9	2.1	33.6	27.1	336.9	1016.5	337.1	25.4
8	68.6	2.5	25.0	2.1	33.4	27.1	336.8	1016.3	337.3	25.3
9	68.8	2.8	25.0	2.4	33.6	27.1	336.9	1016.3	337.4	25.3
10	69.0	2.6	24.9	2.3	33.8	27.1	337.0	1015.9	337.3	25.3
11	68.8	2.2	24.9	2.0	33.6	27.1	336.9	1016.3	337.1	25.3

Table 6 Output responses constrains for minimizing HC emissions and BSFC for Jatropha biodiesel/ diesel blends

	Name	**Goal**	**Lower Limit**	**Upper Limit**
INPUT RESPONSES	LOAD	is in range	40	100
	BLEND	is in range	0	100
	INJECTION TIMING	is in range	18	28
	EGR	is in range	0	20
OUTPUT RESPONSES	SMOKE	is in range	14.36	38
	HC	**Minimize**	**14**	**27.1**
	EGT	None	228	443
	NOx	is in range	581	1031.1
	BSFC	**Minimize**	**312**	**439**
	BTE	None	25	28.6

Table 7. Solutions to the response constrains for minimizing HC emissions and BSFC for diesel/ jatropha biodiesel blends.

No.	LOAD	BLEND	INJECTION TIMING	EGR	SMOKE	HC	EGT	NOx	BSFC	BTE
1	70.2	11.1	23.7	1.7	33.0	24.1	341.4	1031.1	349.9	24.8
2	70.1	11.2	23.8	1.7	32.9	24.1	341.4	1031.1	349.9	24.8

3	70.1	11.0	23.7	1.6	33.0	24.1	341.4	1031.1	349.9	24.8
4	70.3	11.1	23.7	1.7	33.1	24.1	341.4	1031.1	349.9	24.8
5	70.3	11.2	23.7	1.7	33.1	24.1	341.5	1031.1	349.9	24.8
6	70.0	11.0	23.8	1.6	32.8	24.1	341.3	1031.1	349.8	24.8

Table 8. Output responses constrains for minimizing smoke for Jatropha biodiesel/diesel blends

	Name	Goal	Lower Limit	Upper Limit
INPUT RESPONSES	LOAD	is in range	40	100
	BLEND	is in range	0	100
	INJECTION TIMING	is in range	18	28
	EGR	is in range	0	20
OUTPUT RESPONSES	**SMOKE**	**minimize**	**14.3**	**38**
	HC	is in range	14	27.1
	EGT	none	228	443
	NOx	is in range	581	1031.1
	BSFC	is in range	312	439
	BTE	none	25	28.6

Table 9 Solutions to the response constrains for minimizing smoke for Jatropha biodiesel/diesel blends

No.	LOAD	BLEND	INJECTION TIMING	EGR	SMOKE	HC	EGT	NOx	BSFC	BTE
1	49.7	56.0	28.0	2.3	17.0	19.4	327.6	1031.1	439.0	21.6
2	49.6	55.3	28.0	2.0	17.0	19.3	327.9	1031.1	439.0	21.6
3	49.6	55.0	28.0	1.9	17.0	19.3	328.1	1031.1	439.0	21.6
4	49.7	56.7	28.0	2.6	17.0	19.4	327.1	1031.1	439.0	21.7
5	49.7	55.8	28.0	2.2	17.0	19.4	327.7	1031.1	439.0	21.6
6	49.6	54.8	28.0	1.8	17.0	19.3	328.2	1031.1	439.0	21.6
7	49.8	57.2	28.0	2.8	17.0	19.5	326.8	1031.1	439.0	21.7
8	49.5	54.3	28.0	1.6	17.0	19.3	328.5	1031.1	438.9	21.6
9	49.8	57.8	28.0	3.0	17.0	19.5	326.5	1031.1	439.0	21.7
10	49.9	57.2	28.0	2.7	17.0	19.4	326.8	1030.9	439.0	21.7
11	49.4	52.8	28.0	1.0	17.1	19.2	329.2	1031.0	439.0	21.5
12	49.5	53.2	28.0	1.1	17.1	19.2	329.0	1031.1	439.0	21.5
13	49.9	57.1	27.9	2.6	17.1	19.3	327.0	1031.1	439.0	21.7
14	50.0	56.3	27.8	2.2	17.1	19.2	327.5	1031.1	439.0	21.6
15	50.0	59.4	28.0	3.7	17.1	19.7	325.5	1031.1	439.0	21.7
16	49.3	51.9	28.0	0.6	17.1	19.1	329.6	1031.1	439.0	21.5
17	49.3	51.5	28.0	0.5	17.1	19.1	329.8	1031.1	439.0	21.5

18	49.9	56.6	28.0	2.8	17.1	19.5	327.2	1031.1	437.9	21.7
19	49.7	54.0	28.0	1.7	17.1	19.3	328.6	1031.1	437.8	21.6

Table 10 Output responses constrains for minimizing HC emissions and maximizing BTE for Karanja biodiesel/ diesel blends

	Name	**Goal**	**Lower Limit**	**Upper Limit**
INPUT RESPONSES	LOAD	is in range	40	100
	BLEND	is in range	0	100
	INJECTION TIMING	is in range	18	28
	EGR	is in range	0	20
OUTPUT RESPONSES	SMOKE	is in range	16.1	40
	HC	**minimize**	**14**	**28**
	EGT	none	222	436
	NOx	is in range	581	1015
	BSFC	is in range	312	456
	BTE	**maximize**	**14.4**	**27.9**

Table 11 Solutions to the response constrains for minimizing HC emissions and maximizing BTE for Karanja biodiesel/ diesel blends.

No.	**LOAD**	**BLEND**	**INJECTION TIMING**	**EGR**	**SMOKE**	**HC**	**EGT**	**NOx**	**BSFC**	**BTE**
1	67.0	55.0	21.3	3.1	30.0	17.8	324.5	1015.0	440.9	21.8
2	66.9	55.0	21.4	3.0	29.9	17.8	324.4	1015.0	440.8	21.8
3	66.9	55.4	21.4	3.1	29.9	17.8	324.2	1015.0	441.5	21.8
4	67.0	55.0	21.4	3.1	30.0	17.8	324.5	1015.0	440.7	21.8
5	66.9	54.6	21.4	2.9	29.9	17.9	324.7	1015.0	440.0	21.8
6	67.2	54.8	21.3	3.1	30.3	17.8	324.6	1015.0	440.8	21.8
7	67.2	55.6	21.2	3.2	30.2	17.7	324.1	1015.0	442.2	21.8
8	67.3	53.9	21.3	3.0	30.3	17.9	325.1	1015.0	439.2	21.8
9	67.2	53.9	21.3	2.9	30.1	17.9	325.1	1015.0	439.3	21.8
10	67.2	53.8	21.4	3.1	30.2	18.0	325.1	1015.0	438.7	21.8
11	67.1	56.3	21.2	3.2	30.1	17.7	323.7	1015.0	443.5	21.7
12	66.9	53.7	21.4	2.8	29.8	18.0	325.2	1015.0	438.5	21.8
13	67.0	56.2	21.3	3.4	30.0	17.8	323.8	1015.0	442.7	21.8
14	66.7	56.3	21.4	3.2	29.8	17.8	323.7	1015.0	442.7	21.8
15	67.2	53.4	21.4	2.9	30.2	18.0	325.4	1015.0	438.0	21.9
16	67.2	56.3	21.2	3.4	30.2	17.7	323.7	1015.0	443.2	21.7
17	67.2	54.6	21.2	2.8	30.1	17.8	324.7	1015.0	440.9	21.8
18	66.7	54.0	21.5	2.7	29.6	18.0	325.0	1015.0	438.9	21.8
19	66.6	54.7	21.4	2.7	29.6	17.9	324.6	1015.0	440.3	21.8
20	67.2	56.8	21.2	3.3	30.2	17.6	323.4	1015.0	444.4	21.7

21	67.1	55.1	21.4	3.5	30.2	17.9	324.4	1015.0	440.6	21.8
22	66.7	53.6	21.6	2.8	29.6	18.0	325.2	1015.0	437.8	21.9
23	66.7	57.3	21.4	3.4	29.7	17.7	323.1	1015.0	444.4	21.7
24	67.4	56.5	21.1	3.4	30.5	17.6	323.6	1015.0	444.2	21.7
25	67.0	52.9	21.4	2.5	29.9	18.0	325.6	1015.0	437.4	21.9

Table 12 Output responses constrains for minimizing smoke maximizing BTE for Karanja biodiesel/ diesel blends.

	Name	Goal	Lower Limit	Upper Limit
INPUT RESPONSES	LOAD	is in range	40	100
	BLEND	is in range	0	100
	INJECTION TIMING	is in range	18	28
	EGR	is in range	0	20
OUTPUT RESPONSES	**SMOKE**	**minimize**	**16.1**	**40**
	HC	is in range	14	28
	EGT	none	222	436
	NOx	is in range	581	1015
	BSFC	is in range	312	456
	BTE	**maximize**	**14.4**	**27.9**

Table 13 Solutions to the response constrains for minimizing smoke emissions and maximizing BTE for Karanja biodiesel/diesel blends.

NO.	LOAD	BLEND	INJECTION TIMING	EGR	SMOKE	HC	EGT	NOx	BSFC	BTE
1	58.0	10.9	28.0	0.0	25.8	25.6	333.2	1015.0	369.5	24.1
2	57.8	11.4	28.0	0.0	25.7	25.5	333.2	1015.0	370.5	24.0
3	58.1	10.3	28.0	0.0	25.9	25.7	333.2	1015.0	368.2	24.1
4	57.7	12.0	28.0	0.0	25.6	25.4	333.1	1015.0	371.8	24.0
5	58.3	9.6	28.0	0.0	26.1	25.9	333.2	1015.0	366.4	24.2
6	57.5	12.9	28.0	0.0	25.4	25.2	333.1	1015.0	373.7	23.9
7	57.8	11.6	28.0	0.1	25.7	25.5	333.1	1015.0	370.7	24.0
8	57.7	12.1	28.0	0.2	25.6	25.4	333.1	1014.7	371.8	24.0
9	57.2	13.9	28.0	0.0	25.1	25.0	333.1	1015.0	376.1	23.8
10	58.2	10.8	28.0	0.0	25.9	25.6	333.2	1015.0	368.8	24.1
11	58.9	7.5	28.0	0.1	26.6	26.3	333.1	1015.0	361.8	24.4
12	59.1	7.0	28.0	0.0	26.7	26.4	333.1	1015.0	360.7	24.4
13	57.9	12.5	27.9	0.0	25.6	25.3	333.3	1015.0	372.1	23.9
14	57.7	12.8	28.0	0.7	25.6	25.5	332.9	1015.0	372.2	23.9
15	57.4	12.2	28.0	0.0	25.5	25.4	332.8	1012.2	373.2	23.9
16	57.3	14.6	27.9	0.0	25.1	24.9	333.2	1015.0	376.7	23.8
17	58.7	8.8	28.0	0.5	26.5	26.2	333.0	1014.8	363.8	24.3
18	56.6	16.3	28.0	0.0	24.6	24.6	332.9	1014.8	381.5	23.6
19	58.1	11.8	28.0	0.9	25.9	25.8	332.9	1015.0	369.4	24.1
20	56.5	16.9	28.0	0.1	24.5	24.6	332.9	1015.0	382.5	23.5

21	58.3	11.9	27.8	0.0	25.9	25.4	333.4	1015.0	370.1	24.0
22	58.7	9.3	28.0	0.7	26.4	26.2	333.0	1015.0	364.4	24.3
23	56.5	17.3	28.0	0.0	24.5	24.4	332.9	1015.0	383.3	23.5
24	57.2	15.9	28.0	1.6	25.3	25.3	332.5	1015.0	377.0	23.8
25	56.0	19.4	28.0	0.6	24.2	24.3	332.5	1015.0	386.7	23.4
26	57.3	10.7	28.0	0.0	25.7	25.7	332.0	1005.8	371.9	23.9
27	60.3	2.9	28.0	0.0	27.7	27.2	333.0	1015.0	351.7	24.8
28	58.8	11.9	27.8	0.9	26.3	25.7	333.2	1015.0	367.9	24.1
29	56.5	13.6	28.0	0.0	25.1	25.2	331.9	1005.6	378.5	23.7
30	58.0	7.3	28.0	0.0	26.5	26.4	331.7	1003.5	365.1	24.2

4. PREDICTIVE MODELING OF OUTPUT RESPONSES USING ARTIFICIAL NEURAL NETWORK (ANN)

Dr. Robert Hecht-Neilson, who developed the first neurocomputer, defines an artificial neural network (ANN) as "a computing system consisting of interconnected processing components that process information based on their dynamic state response to external inputs." In practical terms, neural networks are nonlinear statistical modeling tools used to model complex input-output relationships or identify patterns in data. They are massively parallel distributed processors with a natural ability to store and use experiential data as needed. By simulating the functioning of human brain neurons and dendrites using wires and silicon, ANN demonstrates similarities to the human brain in two ways:

(i) acquiring knowledge through a training process or learning, and
(ii) using inter-neuron connection strength, known as synaptic weights, to store knowledge [41,42].

ANN acquires knowledge by learning from pre-recorded experimental data. When a mechanism's operation is excessively complex or expensive, ANN can be a useful tool. In recent years, ANN techniques have been employed to predict internal combustion engine (IC) characteristics [41-50].

This study employed ANN to predict six output responses using four input parameters. The input parameters were Fuel blend, Load, Injection timing, and EGR, and the projected responses were BSFC, BTE, smoke opacity, HC emissions, EGT, and NOx. Table 14 presents the various levels and values of the input parameters for Jatropha and Karanja diesel/biodiesel blends, and all the fuels evaluated shared the same input parameters. The Neuro Intelligence software was used for training, and multilayer perception (MLP) was used for output prediction based on the input parameters for the current design and modelling work.

A sophisticated approach was utilized to train individual MLPs for each engine output response. This allowed for each MLP to have a unique network design, which enhanced its ability to focus on its particular task and improve the accuracy of approximations. Six MLPs were developed, each corresponding to a specific engine output response, with six input neurons in the input layer and one output neuron in the output layer. Figure 29 illustrates a general schematic of a multilayer neural network used to forecast engine responses. The Levenberg-Marquardt algorithm was employed for training, with the hidden layer using a logistic sigmoid activation function and the output neuron utilizing a linear activation function.

To determine the number of hidden layers and neurons in each layer, an architectural search method was employed, and only one hidden layer was used for each MLP to avoid falling into undesirable local minima. The performance of the artificial neural network (ANN) was evaluated using two metrics: Regression Value (R^2) and Absolute Relative Error (ARE). The input engine parameters and output responses were standardized to maximize the total variance in the data, resulting in faster learning. Specifically, the data was scaled from -1 to +1. The absolute relative error (ARE) and regression value (R^2) are calculated as follows:

Figure 29. Schematic of a Multilayer Neural Network

$$R^2 = 1 - \frac{\sum_j (TV_j - OV_j)^2}{\sum_j (OVo_j)^2} \quad (22)$$

$$ARE = \frac{TV - OV}{OV} \times 100 \quad (23)$$

Where, TV is the target value and OV is the output value.

Three different data sets were used for ANN modeling: a training data set, a validation data set, and a test data set. The training data set was used to adjust the weights of the neural networks during training, while the validation data set was utilized to fine-tune network architecture or network parameters other than weights, as well as to stop training if the network performance on the validation data set did not improve. The Neuro Intelligence software employed the validation set to determine the generalization loss and retain the best network, which is the one with the lowest error on the validation set. Table 14 shows that there was a total of 108 data points available for biodiesel and diesel fuel blends, which were divided into a training set (80 data points), a validation set (14 data points), and a test set (14 data points). In all of the networks, the training performance mean square error (MSE) was set to 0.0001 to ensure high accuracy.

Table. 14 Total number of input data set for all the fuels tested.

DATA POINT	LOAD	BLEND	INJECTION TIMING	EGR
1	40	0	18	0
2	70	0	18	0
3	100	0	18	0
4	40	20	18	0
5	70	20	18	0
6	100	20	18	0
7	40	50	18	0
8	70	50	18	0
9	100	50	18	0
10	40	100	18	0
11	70	100	18	0
12	100	100	18	0
13	40	0	23	0
14	70	0	23	0
15	100	0	23	0
16	40	20	23	0
17	70	20	23	0
18	100	20	23	0
19	40	50	23	0
20	70	50	23	0
21	100	50	23	0
22	40	100	23	0
23	70	100	23	0
24	100	100	23	0
25	40	0	28	0
26	70	0	28	0
27	100	0	28	0
28	40	20	28	0
29	70	20	28	0
30	100	20	28	0
31	40	50	28	0
32	70	50	28	0
33	100	50	28	0

34	40	100	28	0
35	70	100	28	0
36	100	100	28	0
37	40	0	18	10
38	70	0	18	10
39	100	0	18	10
40	40	20	18	10
41	70	20	18	10
42	100	20	18	10
43	40	50	18	10
44	70	50	18	10
45	100	50	18	10
46	40	100	18	10
47	70	100	18	10
48	100	100	18	10
49	40	0	23	10
50	70	0	23	10
51	100	0	23	10
52	40	20	23	10
53	70	20	23	10
54	100	20	23	10
55	40	50	23	10
56	70	50	23	10
57	100	50	23	10
58	40	100	23	10
59	70	100	23	10
60	100	100	23	10
61	40	0	28	10
62	70	0	28	10
63	100	0	28	10
64	40	20	28	10
65	70	20	28	10
66	100	20	28	10
67	40	50	28	10
68	70	50	28	10
69	100	50	28	10
70	40	100	28	10
71	70	100	28	10
72	100	100	28	10
73	40	0	18	20
74	70	0	18	20
75	100	0	18	20
76	40	20	18	20
77	70	20	18	20
78	100	20	18	20
79	40	50	18	20
80	70	50	18	20
81	100	50	18	20
82	40	100	18	20
83	70	100	18	20
84	100	100	18	20

85	40	0	23	20
86	70	0	23	20
87	100	0	23	20
88	40	20	23	20
89	70	20	23	20
90	100	20	23	20
91	40	50	23	20
92	70	50	23	20
93	100	50	23	20
94	40	100	23	20
95	70	100	23	20
96	100	100	23	20
97	40	0	28	20
98	70	0	28	20
99	100	0	28	20
100	40	20	28	20
101	70	20	28	20
102	100	20	28	20
103	40	50	28	20
104	70	50	28	20
105	100	50	28	20
106	40	100	28	20
107	70	100	28	20
108	100	100	28	20

The ANN network was used to analyze the performance of Jatropha biodiesel, Karanja biodiesel and their blends with petroleum diesel. The network was trained, validated, and tested on all six output responses. Figures 30-47 show the findings for Jatropha biodiesel/diesel blends, with the BSFC, BTE, Smoke emissions, Unburnt HC emissions, EGT, and NOx emissions training, validation, and testing plots depicted. The MLP's hidden layer had 11 neurons for BSFC and 14 neurons for BTE. The regression values were 0.997 for BSFC, 0.981 for BTE, 0.976 for smoke emissions, 0.966 for unburnt HC emissions, 0.976 for EGT, and 0.996 for NOx emissions, indicating high training and prediction skills. The analysis for Karanja is identical, and the results can be plotted similarly and has not been described because it would be redundant, with the only variation being the regression values.

Figure 30. Network s plot of BSFC for Jatropha biodiesel and its blends

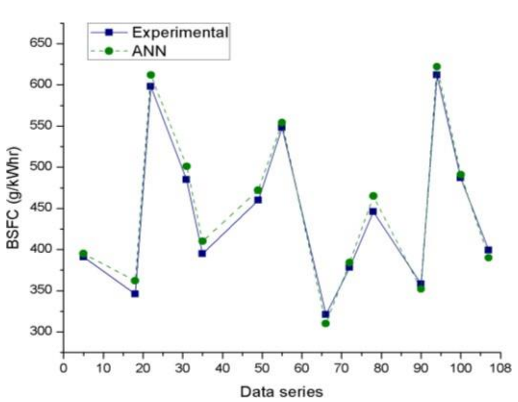

Figure 31. Network validation plot of BSFC for Jatropha biodiesel and its blends.

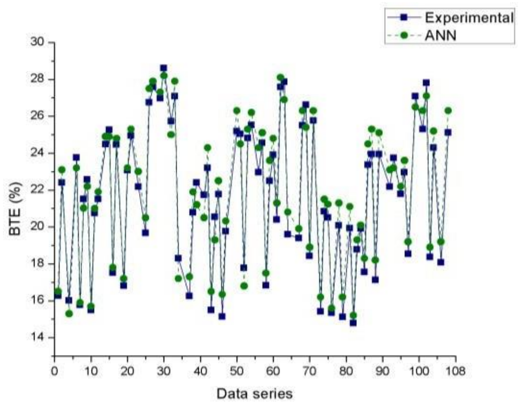

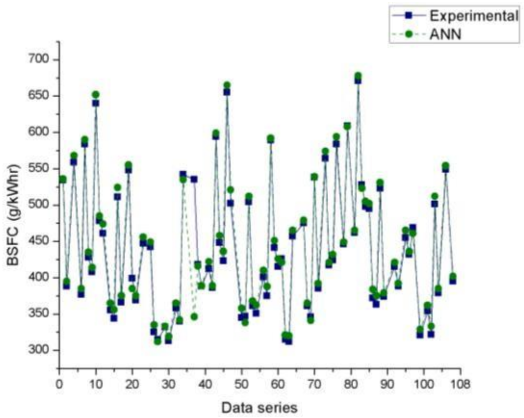

Figure 32. Network Testing plot of BSFC for Jatropha biodiesel and its blends.

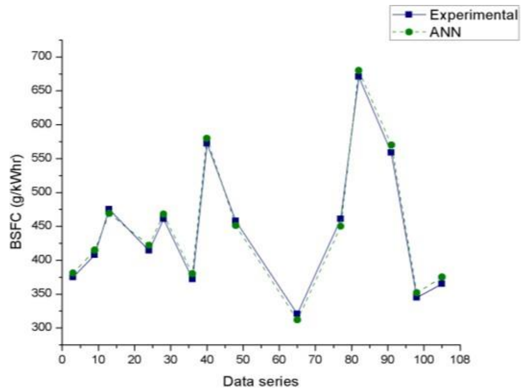

Figure 33. Network Training plot of BTE for Jatropha biodiesel and its blends

\

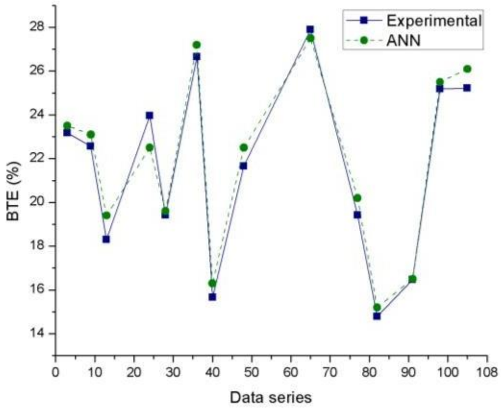

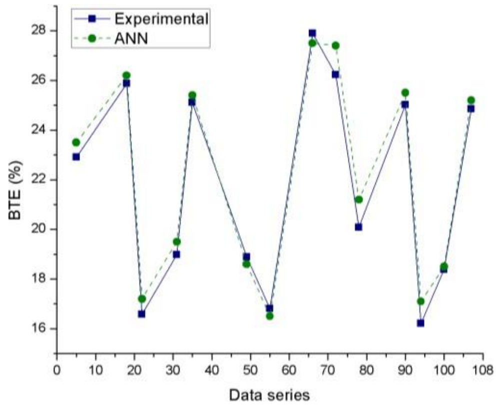

Figure 34. Network Validation plot of BTE for Jatropha biodiesel and its blends

Figure 35. Network Testing plot of BTE for Jatropha biodiesel and its blends

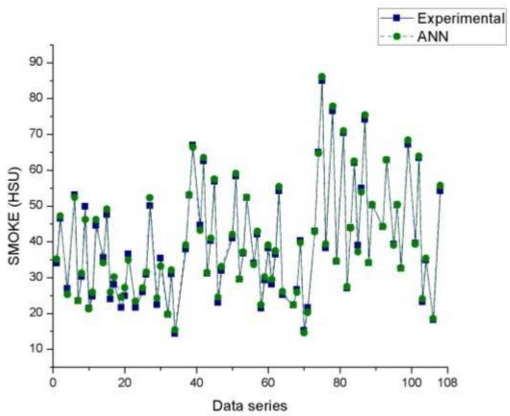

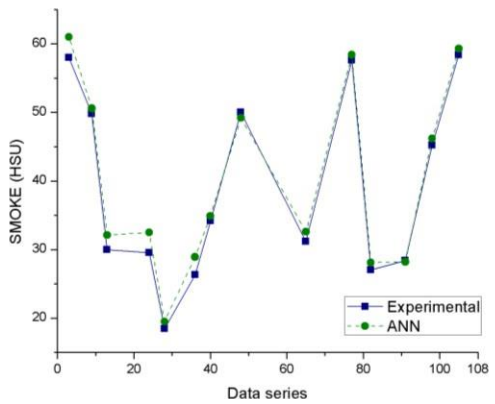

Figure 36. Network Training plot of Smoke opacity for Jatropha biodiesel and its blends

Figure 37. Network Validation plot of Smoke opacity for Jatropha biodiesel and its blends

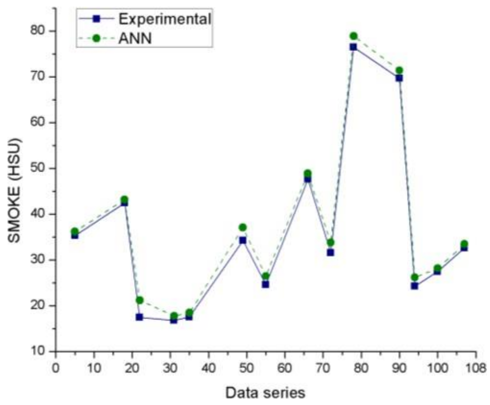

Figure 38. Network Testing plot of Smoke opacity for Jatropha biodiesel and its blends

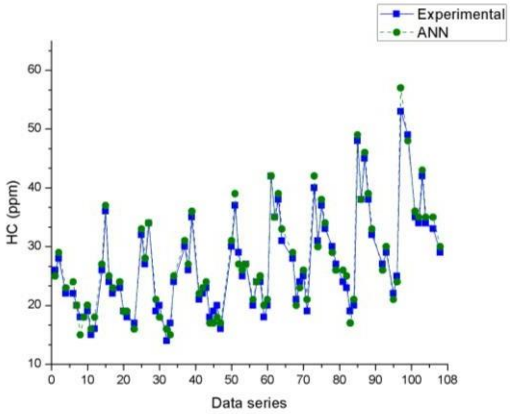

Figure 39. Network Training plot of UBHC for Jatropha biodiesel and its blends

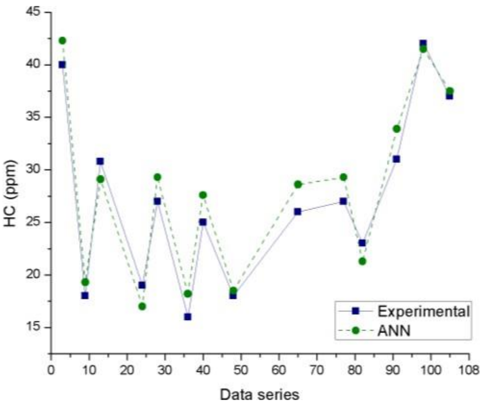

Figure 40. Network Validation plot of UBHC for Jatropha biodiesel and its blends

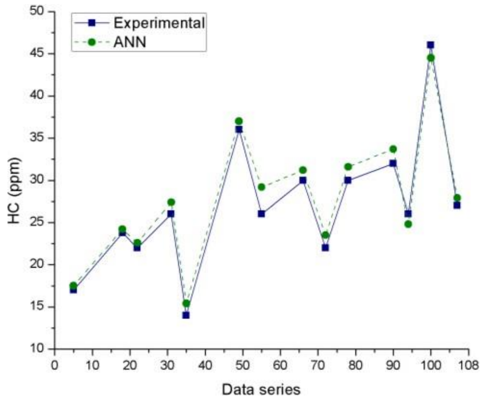

Figure 41. Network Testing plot of UBHC for Jatropha biodiesel and its blends

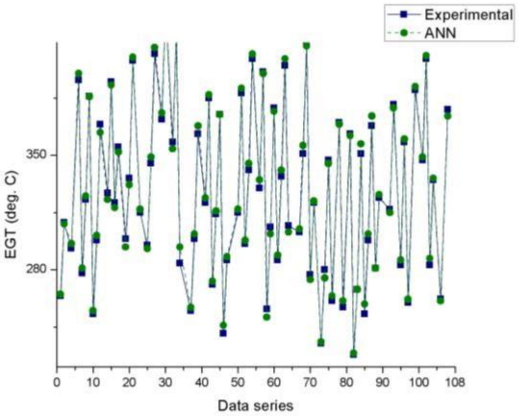

Figure 42. Network Training plot of EGT for Jatropha biodiesel and its blends

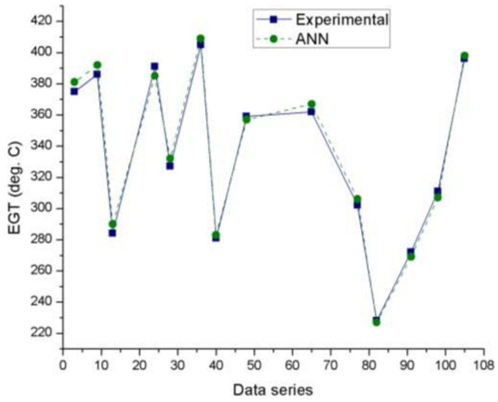

Figure 43. Network Validation plot of EGT for Jatropha biodiesel and its blends

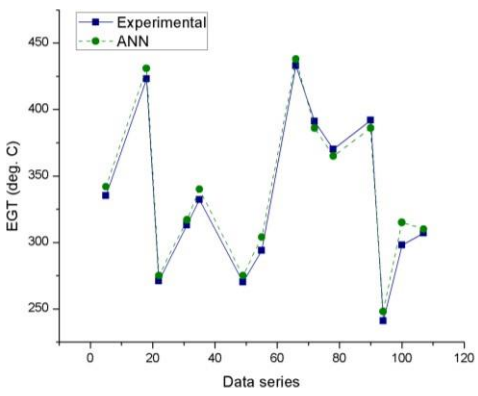

Figure 44. Network Testing plot of EGT for Jatropha biodiesel and its blends

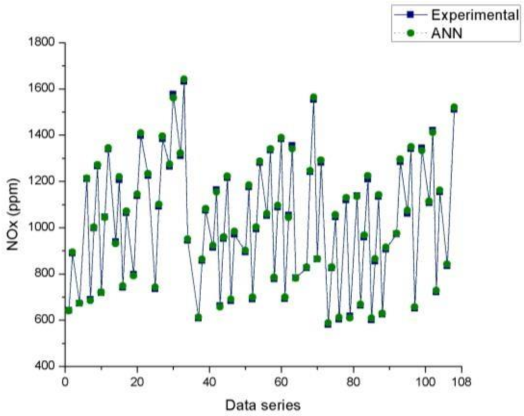

Figure 45. Network Training plot of NOx for Jatropha biodiesel and its blends

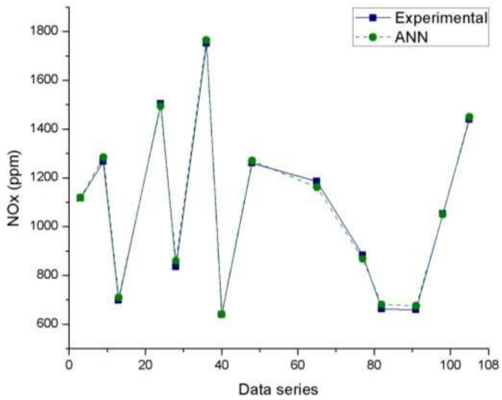

Figure 46. Network Training plot of NOx for Jatropha biodiesel and its blends

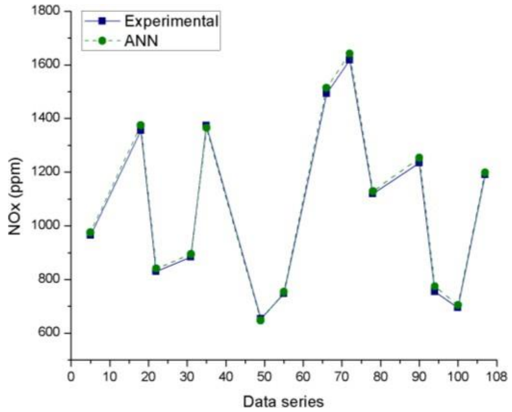

Figure 47. Network Testing plot of NOx for Jatropha biodiesel and its blends

The ANN models utilized in this study exhibited exceptional performance across all three data sets: training, validation, and testing. Their regression values indicate that the MLPs were able to effectively predict and train with a high degree of accuracy, demonstrating strong training and prediction capabilities. While there was a slight decrease in performance for HC emissions in both biodiesel fuels, the overall results were highly satisfactory. In fact, the ANN modelling approach successfully predicted engine output responses for both fuels, based on six different engine control parameters. These impressive findings demonstrate the potential of ANN models to accurately forecast and optimize engine performance, making them a valuable tool in the field of engineering.

6. CONCLUSIONS

This study examines the fuel economy, performance, and emissions of biodiesel and its blends on a small diesel engine. Using Jatropha Curcas and Pongamia Pinnata as sources, the performance and emissions analysis was done on Kirloskar make CAF1 constant speed (1500 rpm), single cylinder DI engine having rated power of 4.5 kW.

•The study found that diesel has better thermal efficiency at low loads, but the 20% blend of Jatropha (JB20) performed slightly better at high loads. The results suggest that biodiesel blends have the potential to outperform diesel in certain conditions in terms of the efficiency.

• The study found the decrease in BSFC was more significant when increasing the load from 40% to 70% due to increased efficiency and reduced friction to brake power. However, at higher loads, the reduction in BSFC was minimal due to a decrease in fuel conversion efficiency. The study also found that injection timing had a significant impact on BSFC, with early combustion resulting in a 7-12% reduction in BSFC, while retarding injection caused a 7-14% increase in BSFC due to lower effective pressure during the working stroke.

• Adding biodiesel to diesel reduces smoke emissions due to the presence of oxygen. Jatropha biodiesel outperforms Karanja biodiesel in reducing smoke emissions due to its lower viscosity and smaller droplet size. Increased load results in higher smoke opacity due to the formation of a rich fuel-air mixture at high loads. Advancing injection start by 50 lowers smoke by 6-18%, while retarding it by 50 increases smoke opacity by 10-22%.

• Biodiesel use increases NOx emissions due to its high cetane number and free oxygen content. JB100 and KB100 had 24% and 19% higher NOx emissions than diesel at full load and adding 20% biodiesel increases NOx by 4-6% at 40% load and 8-12% at full load. Jatropha biodiesel produces higher NOx due to higher combustion temperatures than Karanja biodiesel. All fuels exhibit increased NOx emissions when load is increased from 40% to 100% and advancing injection timing from 230 btdc to 280 btdc increases NOx by 14%-17.8%, while retarding it reduces NOx emissions by 5-15%.

• HC emissions decrease as the biodiesel concentration in a blend is increased. Karanja biodiesel and blends have higher HC emissions due to higher viscosity. HC emissions for all fuels decrease when load increases from 40% to 70%, and injection timing advanced by 5^{o} decreases HC emissions up to 41%, while retarding it increases HC emissions up to 23%.

• Smoke level increases with increased exhaust gas in the intake as exhaust gas recirculation dilutes the inlet air, decreasing oxygen concentration. Reduced oxygen concentration leads to fuel burning in fuel-rich regions, resulting in smoke formation. The impact of exhaust gas recirculation on smoke levels is smaller for biodiesel and their blends than diesel, as JME contains oxygen, which aids in soot oxidation.

• HC emissions increase with increased exhaust gas recirculation for both fuels, as intake mixture dilution leads to a locally rich mixture, resulting in slower reactions and incomplete combustion products. CO_2 in the intake mixture lowers temperature and pressure at a given volume, leading to longer ignition delay periods and higher HC emissions. At full load, the variation in HC emissions with exhaust gas recirculation is linear for all fuels.

• Increasing the percentage of exhaust gas recirculation (EGR) in the inlet was found to significantly reduce NOx emissions. This is because EGR dilutes the inlet air, decreasing oxygen concentration and increasing heat capacity of the inlet charge, ultimately leading to a reduction in NOx formation. However, it was observed that the reduction in NOx emissions was more significant at low load (40% of rated load) than at high load (100% of rated load). On the other hand, increasing EGR from 0% to 20% resulted in increased brake specific fuel consumption (BSFC) for all fuels due to decreased oxygen concentration in the inlet mixture, which limits complete fuel combustion. The effect of EGR on BSFC was less pronounced at 40% load for all fuels, and the impact on diesel was greater than on biodiesel or their blends due to the presence of oxygen content in the latter.

• Response surface methodology (RSM) was found to be a useful technique for modelling engine responses using four input parameters viz. blend percentage, load, injection timing and EGR. For Jatropha biodiesel and blends, R2 values of the fitted RSM models for BSFC, BTE, smoke, HC and NOx were 0.99, 0.98, 0.98, 0.93 and 0.99 respectively, whereas for Karanja biodiesel and blends, the corresponding R2 values were found to be 0.98, 0.98, 0.98, 0.94 and 0.98.

• Based on multi objective optimization and contour plots, various pareto-optimal solutions were obtained for various required input values for the desired output constraints.

• Prediction of engine responses as a function of operating, injection system parameters and exhaust gas recirculation using neural network approach was found to be meaningful. For testing, good approximation were obtained for all responses for both the fuels.

Data Availability Statement

The data that support the findings of this study are available from the author, Professor Rajesh Kumar Saluja upon reasonable request.

REFERENCES

[1] Wongjaikham, W., Wongsawaeng, D., Ratnitsai, V., Kamjam, M., Ngaosuwan, K., Kiatkittipong, W., Hosemann, P. and Assabumrungrat, S.: Low-cost alternative biodiesel production apparatus based on household food blender for continuous biodiesel production for small communities. Scientific reports, 11(1) 13827 (2021)

[2] Silverman, D.T., Samanic, C.M., Lubin, J.H., Blair, A.E., Stewart, P.A., Vermeulen, R., Coble, J.B., Rothman, N., Schleiffm, P. L., Travis, W. D., Ziegler, R. G..: The diesel exhaust in miners study: a nested case–control study of lung cancer and diesel exhaust. Journal of the National Cancer Institute. 104(11):855-68 (2012)

[3] Tirumareddy, P., Esmi, F., Masoumi, S., Borugadda, V.B. and Dalai, A.K.: Introduction to Green Diesel. In Green Diesel: An Alternative to Biodiesel and Petrodiesel, Singapore: Springer Nature Singapore, 1-40 (2022)

[4] Aslan, Volkan. "An Overview of Biodiesel Produced from 2nd Generation Feedstock: Mustard Seed Types." BioEnergy Research (2022): 1-21.

[5] Mishra, V.K., Goswami, R.: A review of production, properties and advantages of biodiesel. Biofuels. 9(2), 273-89, (2018)

[6] Prasad, S., Kumar, S., Sheetal, K.R. and Venkatramanan, V.: Global climate change and biofuels policy: Indian perspectives. Global climate change and environmental policy: Agriculture perspectives, 207-226 (2020)

[7] Kaisan, M.U., Abubakar, S., Ashok, B., Balasubramanian, D., Narayan, S., Grujic, I., Stojanovic, N.: Comparative analyses of biodiesel produced from jatropha and neem seed oil using a gas chromatography–mass spectroscopy technique. Biofuels. (2018)

[8] Rezania, S., Oryani, B., Park, J., Hashemi, B., Yadav, K. K., Kwon, E. E., Cho, J. : Review on transesterification of non-edible sources for biodiesel production with a focus on economic aspects, fuel properties and by-product applications. Energy Conversion and Management, 201, 112155 (2019)

[9] Sharma, A., Pali, H.S., Kumar, M., Singh, N.K., Singh, Y. and Singh, D.: Study the effect of optimized input parameters on a CRDI diesel engine running with waste frying oil methyl ester-diesel blend fuel with ZnO nanoparticles: a response surface methodology approach. Biomass Conversion and Biorefinery, 1-26 (2022)

[10] Babu, D., and R. Anand.: Biodiesel-diesel-alcohol blend as an alternative fuel for DICI diesel engine. In Advanced biofuels, pp. 337-367. Woodhead Publishing (2019)

[11] Datta, A., Mandal, B.K.: Use of Jatropha biodiesel as a future sustainable fuel. Energy Technology & Policy. 1(1):8-14 (2014)

[12] Nutakki, P.K., Gugulothu, S.K., Ramachander, J. and Sivasurya, M.: Effect Of n-amyl alcohol/biodiesel blended nano additives on the performance, combustion and emission characteristics of CRDi diesel engine. Environmental Science and Pollution Research, 1-16 (2021)

[13] Devarajan, Y., Munuswamy, D.B., Radhakrishnan, S., Mahalingam, A., Nagappan, B.: Experimental testing and evaluation of neat biodiesel and heptanol blends in diesel engine. ASTM International (2019)

[14] Ağbulut, Ü., Sarıdemir, S. and Albayrak, S.: Experimental investigation of combustion, performance and emission characteristics of a diesel engine fuelled with diesel–biodiesel–alcohol blends. Journal of the Brazilian Society of Mechanical Sciences and Engineering, 41, 1-12 (2019)

[15] Patidar, S.K., Raheman, H.: Performance and durability analysis of a single-cylinder direct injection diesel engine operated with water emulsified biodiesel-diesel fuel blend. Fuel. 273, 117779. (2020)

[16] Paul, G., Datta, A., Mandal, B.K.: An experimental and numerical investigation of the performance, combustion and emission characteristics of a diesel engine fueled with jatropha biodiesel. Energy Procedia. 54, 455-67. (2014)
[17] Rangabashiam, D.: Investigation on the performance, emission and combustion pattern of research diesel engine fueled with higher alcohol and pongamia biodiesel blends. Energy Sources, Part A: Recovery, Utilization, and Environmental Effects. (2019)
[18] Sham, R., Saluja, R.K., Singh, G., Kumar, V., Parmar, S.: Experimental investigation to study the effects of using hot and partially cold EGR in direct injection diesel engine. Technology. 4(03), 170-173 (2016)
[19] Kumar, V., Mahla, S.K.: Influence of EGR on a CI engine running on 20% blend of jatropha biodiesel. Materials Today: Proceedings. 43, 273-80 (2021)
[20] Kodate, S.V., Yadav, A.K. and Kumar, G.N.: Combustion, performance and emission analysis of preheated KOME biodiesel as an alternate fuel for a diesel engine. Journal of Thermal Analysis and Calorimetry, 141, 2335-2345 (2020)
[21] Folaranmi, J.: Production of biodiesel (B100) from Jatropha oil using sodium hydroxide as catalyst. Journal of Petroleum Engineering. (2012)
[22] Teo, S.H., Islam, A., Chan, E.S., Choong, S.T., Alharthi, N.H., Taufiq-Yap, Y.H., Awual, M.R.: Efficient biodiesel production from Jatropha curcus using CaSO4/Fe2O3-SiO2 core-shell magnetic nanoparticles. Journal of cleaner production. 208, 816-26 (2019)
[23] Singh, A., Sinha, S., Choudhary, A.K., Chelladurai, H.: Biodiesel production using heterogeneous catalyst, application of Taguchi robust design and response surface methodology to optimise diesel engine performance fuelled with Jatropha biodiesel blends. International Journal of Ambient Energy. (2020)
[24] Shameer, P.M., Ramesh, K. FTIR assessment and investigation of synthetic antioxidant on the fuel stability of Calophyllum inophyllum biodiesel. Fuel. 209, 411-16. (2017)
[25] Saluja, R.K., Kumar, V., Sham, R.: Stability of biodiesel–A review. Renewable and Sustainable Energy Reviews. 62, 866-81 (2016)
[26] Singh, N., Kaushal, R, Saluja, R.K.: Storage Stability Analysis of Biodiesel Prepared from Jatropha Oil. Jour of Adv Research in Dynamical & Control Systems, 11, 01-Special Issue, (2019)
[27] Acherki, H., Bouaid, A., Marchetti, J.M.: Optimization of the enzymatic butanolysis of jatropha oil for biodiesel production using Eversa. Biofuels, Bioproducts and Biorefining. (2022)
[28] Gul, M., Shah, A.N., Aziz, U., Husnain, N., Mujtaba, M.A., Kousar, T., Ahmad, R., Hanif, M.F.: Grey-Taguchi and ANN based optimization of a better performing low-emission diesel engine fueled with biodiesel. Energy Sources, Part A: Recovery, Utilization, and Environmental Effects (2019)
[29] Zulfiqar, A., Mumtaz, M.W., Mukhtar, H., Najeeb, J., Irfan, A., Akram, S., Touqeer, T., Nabi, G.: Lipase-PDA-TiO2 NPs: An emphatic nano-biocatalyst for optimized biodiesel production from Jatropha curcas oil. Renewable Energy. 169:1026-37 (2021)
[30] Mendonça, I.M., Paes, O.A., Maia, P.J., Souza, M.P., Almeida, R.A., Silva, C.C., Duvoisin Jr, S. and de Freitas, F.A.: New heterogeneous catalyst for biodiesel production from waste tucumã peels (Astrocaryum aculeatum Meyer): Parameters optimization study. Renewable Energy. 130, 103-110 (2019)
[31] Yatish, K.V., Lalithamba, H.S., Suresh, R., Hebbar, H.H.: Optimization of bauhinia variegata biodiesel production and its performance, combustion and emission study on diesel engine. Renewable Energy. 122:561-75 (2018)
[32] Kamel, D.A., Farag, H.A., Amin, N.K., Zatout, A.A., Ali, R.M.: Smart utilization of jatropha (Jatropha curcas Linnaeus) seeds for biodiesel production: Optimization and mechanism. Industrial Crops and Products. 111, 407-13. (2018)
[33] Shrivastava, K., Thipse, S.S., Patil, I.D.: Optimization of diesel engine performance and emission parameters of Karanja biodiesel-ethanol-diesel blends at optimized operating conditions. Fuel. 293, 120451 (2021)

[34] Singh, A., Sinha, S., Choudhary, A.K., Panchal, H., Elkelawy, M., Sadasivuni, K.K.: Optimization of performance and emission characteristics of CI engine fueled with Jatropha biodiesel produced using a heterogeneous catalyst (CaO). Fuel. 280:118611 (2020)
[35] Singh, R., Bux, F., Sharma, Y.C.: Optimization of biodiesel synthesis from microalgal (Spirulina platensis) oil by using a novel heterogeneous catalyst, β-strontium silicate (β-Sr2SiO4). Fuel. 280, 118312 (2020)
[36] Garg A, Jain S.: Process parameter optimization of biodiesel production from algal oil by response surface methodology and artificial neural networks. Fuel. 277, 118254 (2020)
[37] Agarwal, A.K., Gupta, T., Shukla, P.C., Dhar, A.: Particulate emissions from biodiesel fuelled CI engines. Energy Conversion and Management. 94, 311-30 (2015)
[38] Dincer, K.: Lower emissions from biodiesel combustion. Energy Sources, Part A. 30 (10), 963-68. (2008)
[39] Pereira, L.M., Milan, T.M., Tapia-Blácido, D.R.: Using Response Surface Methodology (RSM) to optimize 2G bioethanol production: A review. Biomass and Bioenergy. 151, 106166. (2021)
[40] Weremfo, A., Abassah-Oppong, S., Adulley, F., Dabie, K., Seidu-Larry, S.: Response surface methodology as a tool to optimize the extraction of bioactive compounds from plant sources. Journal of the Science of Food and Agriculture. 103(1), 26-36 (2022)
[41] Sharma, P., Sahoo, B.B.: Precise prediction of performance and emission of a waste derived Biogas–Biodiesel powered Dual–Fuel engine using modern ensemble Boosted regression Tree: A critique to Artificial neural network. Fuel. 321, 124131 (2022)
[42] Olatunji, O., Akinlabi, S., Madushele, N.: Application of artificial intelligence in the prediction of thermal properties of biomass. In Valorization of Biomass to Value-Added Commodities, Springer, 59-91, 2020
[43] Hoang, A.T., Nižetić, S., Ong, H.C., Tarelko, W., Le, T.H., Chau, M.Q., Nguyen, X.P.: A review on application of artificial neural network (ANN) for performance and emission characteristics of diesel engine fueled with biodiesel-based fuels. Sustainable Energy Technologies and Assessments. 47, 101416 (2021)
[44] Aydın, M., Uslu, S., Çelik, M.B.: Performance and emission prediction of a compression ignition engine fueled with biodiesel-diesel blends: A combined application of ANN and RSM based optimization. Fuel. 269, 117472 (2020)
[45] Onukwuli, D.O., Esonye, C., Ofoefule, A.U., Eyisi, R.: Comparative analysis of the application of artificial neural network-genetic algorithm and response surface methods-desirability function for predicting the optimal conditions for biodiesel synthesis from chrysophyllum albidum seed oil. Journal of the Taiwan Institute of Chemical Engineers. 125, 153-67 (2021)
[46] Tosun, E., Aydin, K., Bilgili, M.: Comparison of linear regression and artificial neural network model of a diesel engine fueled with biodiesel-alcohol mixtures. Alexandria Engineering Journal. 55 (4), 3081-89. (2016)
[47] Lage, C.S., de, Morais, Hanriot, S., Zárate, L.E.: Using artificial neural networks to represent a diesel–biodiesel engine. Journal of the Brazilian Society of Mechanical Sciences and Engineering. 42(11), 1-2. (2020)
[48] Hariram, V., Seralathan, S., KL, V, Micha Premkumar, T.: Performance assessment of artificial neural network on the prediction of Calophyllum inophyllum biodiesel through two-stage transesterification. Energy Sources, Part A: Recovery, Utilization, and Environmental Effects. 2021
[49] Uslu S, Celik MB. Prediction of engine emissions and performance with artificial neural networks in a single cylinder diesel engine using diethyl ether. Engineering science and technology, an international journal. 2018 Dec 1;21(6):1194-201. May 3;43(9):1060-72.
[50] Channapattana SV, Pawar AA, Kamble PG. Optimisation of operating parameters of DI-CI engine fueled with second generation Biofuel and development of ANN based prediction model. Applied energy. 2017 Feb 1; 187:84-95.

[51] Kenanoğlu R, Baltacıoğlu MK, Demir MH, Özdemir ME. Performance & emission analysis of HHO enriched dual-fuelled diesel engine with artificial neural network prediction approaches. International Journal of Hydrogen Energy. 2020 Oct 2;45(49):26357-69.

[52] Hosseini SH, Taghizadeh-Alisaraei A, Ghobadian B, Abbaszadeh-Mayvan A. Artificial neural network modeling of performance, emission, and vibration of a CI engine using alumina nano-catalyst added to diesel-biodiesel blends. Renewable energy. 2020 Apr 1;149:951-61.